Quantum decay rates for dissipative systems at finite temperatures

Hermann Grabert
Service de Physique du Solide, Centre d'Etudes Nucléaires de Saclay, 91191 Gif-sur-Yvette, France

Peter Olschowski and Ulrich Weiss
Institut für Theoretische Physik, Universität Stuttgart, 7000 Stuttgart 80, Germany
(Received 26 March 1987)

The decay of a metastable state of a system coupled to a heat-bath environment is studied. A functional-integral method is presented allowing for the calculation of decay rates at finite temperatures and in the presence of dissipation. The theory is utilized to determine the rate for a wide range of parameters. The temperature extends from the region where the decay is thermally activated down to very low temperatures where the system decays by tunneling from its ground state in the metastable well. The range of damping parameters covers the region from weakly damped to heavily overdamped motions. It is found that the transition between thermally activated decay and tunneling occurs near a crossover temperature T_0 which decreases with increasing damping strength. Well above T_0 the rate follows the classical Arrhenius law where the preexponential factor is affected by the frequency-dependent damping. As T_0 is approached, quantum corrections to the classical rate formula become increasingly important. In the vicinity of T_0 the rate follows a scaling law describing the crossover between thermally activated and quantum-mechanical decay. In the region below T_0 the decay rate can be determined analytically only in limiting cases. For a system with Ohmic dissipation and a cubic potential, accurate numerical calculations are presented exhausting the range of parameters not covered by analytical results.

I. INTRODUCTION

The decay of metastable states in macroscopic systems plays a central role in many areas of physics including low-temperature physics, nuclear physics, and chemical physics. In this paper we investigate the influence of a heat-bath environment on such processes. We aim at accurate analytical and numerical predictions on the temperature dependence of the decay rate covering the range from thermally activated processes at high temperatures down to very low temperatures where the system decays by quantum-mechanical tunneling from the ground state in the metastable well. We also examine a wide range of damping parameters extending from weakly damped to extremely overdamped motions.

This work was partially motivated by an ongoing discussion about the validity of quantum mechanics on a macroscopic scale. Some time ago Leggett argued that quantum mechanics might not be applicable to macroscopic variables and conjectured that corrections to standard quantum theory could perhaps be observable in the rate of transitions between macroscopically distinct states.[1] This has stimulated recent experiments testing quantum effects in the behavior of macroscopic state variables.[2–4] The precise analysis of some of these experiments requires reliable theoretical predictions for the decay rate of a metastable state of a macroscopic system. Here, we present methods and results of such calculations. Parts of this work were published earlier in short form.[5–7] The application of our results to the phenomenon of macroscopic quantum tunneling in Josephson systems[8,9] will be discussed in detail in a subsequent article.[10]

Since microscopic variables interact with a large number of microscopic degress of freedom, the theoretical calculation of transition rates between macroscopically distinct states has to start out from a formulation of quantum mechanics which incorporates the effects of a heat-bath environment. Clearly, the description of dissipation within the framework of quantum theory has extensively been discussed in the literature. For processes involving tunneling, a functional integral formulation of the problem was found to be particularly suitable. The general method was expounded in an article by Caldeira and Leggett.[11] These authors have investigated the influence of frequency-independent damping on the decay rate at zero temperature. Subsequently, many authors have utilized the Caldeira-Leggett approach to supplement and extend the work in various directions[12–23] including finite-temperature calculations, the transition to Arrhenius-type behavior, and the effects of memory damping. Some of these problems were also addressed by alternative methods.[24]

In the present work we shall assume that the system in question can be visualized as a particle of mass M moving in a metastable potential $V(q)$ while coupled to a heat-bath environment. Following Caldeira and Leggett[11] the reservoir is assumed to be representable as a set of harmonic oscillators interacting linearly with the particle. The density and coupling constants of the environmental modes are chosen in such a way that the classical deterministic equation of motion takes the familiar form

$$M\ddot{q}+\frac{\partial V}{\partial q}+M\int_0^t ds\,\gamma(t-s)\dot{q}(s)=0\ , \tag{1.1}$$

where $\gamma(t)$ is a damping kernel with Laplace transform

$$\hat{\gamma}(z)=\int_0^\infty dt\,e^{-zt}\gamma(t)\ . \tag{1.2}$$

When $V(q)$ is a metastable potential of the form depicted in Fig. 1, a particle confined to the metastable region will ultimately escape to the region of lower potential on the other side of the barrier. Naturally, the concept of metastability only makes sense when the barrier is large enough that the decay rate of the metastable state is small compared with other characteristic frequency scales of the problem. Two of those are provided by the curvature of the potential near the metastable minimum and the barrier top. The well frequency

$$\omega_0=[V''(0)/M]^{1/2} \tag{1.3}$$

characterizes the undamped dynamics near the bottom of the well which the system occupies initially in a state of quasiequilibrium. The barrier frequency

$$\omega_b=[-V''(q_b)/M]^{1/2} \tag{1.4}$$

characterizes the width of the parabolic top of the barrier hindering the decay process.

At high temperatures the decay is thermally activated and the rate follows the Arrhenius law

$$\Gamma_{\rm cl}=f_{\rm cl}\exp(-V_b/k_BT) \tag{1.5}$$

where V_b is the barrier height and $f_{\rm cl}$ the classical preexponential factor, sometimes called the attempt frequency. A simplified description of the escape by transition state theory yields for this factor $f_{\rm TST}=\omega_0/2\pi$. In a seminal paper,[25] Kramers has determined the effect of friction on the preexponential factor for a particle subject to frequency independent or Ohmic damping, $\hat{\gamma}(z)=\gamma$, and corresponding Gaussian white noise. In the region of moderate to large damping $f_{\rm cl}$ is reduced as compared to $f_{\rm TST}$ because of diffusive recrossings of the barrier top. On the other hand, for very weak friction, typically $\gamma\lesssim\omega_b k_BT/V_b$, the influence of the heat bath is not strong enough to maintain thermal equilibrium in the metastable well. Because of the depletion of the highly excited states, the preexponential factor decreases linearly with γ. This region of energy diffusion limited classical escape has attracted renewed interest only lately,[26] and attempts were made to bridge between the Kramers limits. Particularly important are recent extensions[27,28] of the Kramers theory for systems with frequency-dependent damping corresponding to a retarded damping term in the classical equation of motion (1.1). Since the barrier frequency ω_b of a metastable system may well be in the GHz region, the difference between the damping strength at that frequency and the zero-frequency Ohmic damping can be quite pronounced leading to significant memory effects.[29]

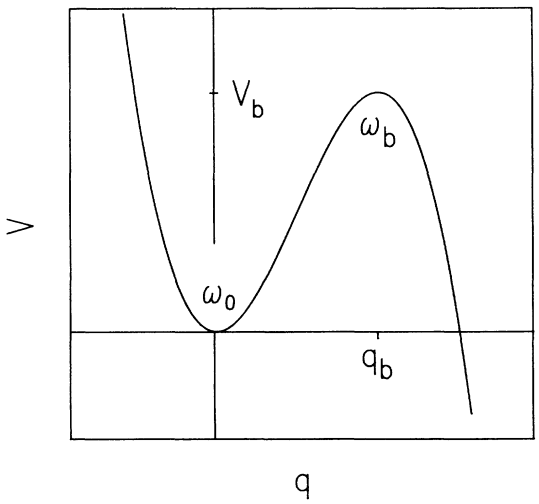

FIG. 1. A metastable potential well.

As the temperature is lowered, the classical escape rate (1.5) decreases exponentially fast so that at very low temperatures the metastable state can only decay via quantum tunneling. A simple criterion for the temperature T_0, where roughly the transition between thermally activated and quantum mechanical decay occurs, was put forward by Goldanski.[30] Equating the Arrhenius factor with the Gamov factor for the penetration of a parabolic barrier, one finds $T_0=\hbar\omega_b/2\pi k_B$. The effect of damping on this crossover temperature was determined only recently.[5,6,13,20] These studies were based on a thermodynamic method for the calculation of decay rates pioneered by Langer.[31] In this approach one calculates the free energy of the metastable system. Because of the states of lower energy on the other side of the barrier, the partition function can only be defined by means of an analytical continuation from a stable potential to the metastable situation depicted in Fig. 1. This procedure leads to an imaginary part of the free energy of the metastable state which then is related to the decay rate of the system in analogy to the interpretation of imaginary energies of resonances in quantum-field theory. An explicit calculation by Affleck[32] for an undamped system has demonstrated that Langer's method yields the same result as a Boltzmann average of energy dependent decay rates. While in the absence of a fully dynamical justification of the approach its range of validity is not exactly known,[33] it is highly suggestive that Langer's method gives the correct result for the decay rate whenever nonequilibrium effects within the metastable well can be neglected. This is the case when the environmental coupling is strong enough in order to maintain thermal equilibrium within the metastable well. In fact, as we have shown previously,[6] the rate formula obtained from the imaginary part of the free energy of a damped system reduces at high temperatures to the classical expression for moderate to large damping. The effects of frequency-dependent damping[27] and the size of quantum corrections to thermally activated decay calculated by dynamical theories[34] are also fully reproduced by the thermodynamic method.[6] On the other hand, the region of energy diffusion limited decay dominated by nonequilibrium effects in the metastable well is not within reach of Langer's method. However, this region, characterized by $\hat{\gamma}(\omega_b)\lesssim\omega_b k_BT/V_b$, is very small in particular for sys-

tems with high barriers.

In the quantum regime the bottleneck of energy activation is absent since the state can decay by tunneling without the help of thermal fluctuations. Consequently, the range of validity of the thermodynamic rate formula is expected to extend to even weaker damping below T_0. In particular, at zero temperature the formula remains valid even for vanishing damping. As a consequence, we are confident that the results presented below give accurate predictions of decay rates for damped metastable systems in the entire temperature range below T_0 (except for exponentially small damping) and also for temperatures above T_0 for moderate to large damping.

Specifically, the thermodynamic rate calculation starts out from a functional integral representation of the free energy which is evaluated in a steepest descent approximation. This simplification is appropriate whenever the rate is exponentially small compared with other relevant frequency scales. Only the region in the vicinity of T_0 needs a more careful treatment (see below). The crossover between thermally activated and quantum-mechanical decay is associated with a change from a trivial saddle-point trajectory to an oscillatory orbit giving the predominant contribution to the imaginary part of the free energy. The calculation of quantum decay rates by Langer's method has developed through the work[35] of Miller, Stone, and Coleman and Callan. Coleman coined the name "bounce" for the oscillatory trajectory which exists only for temperatures below the crossover temperature T_0. In terms of the Euclidean action S_B of this bounce the quantum decay rate reads as

$$\Gamma=\omega_q \exp(-S_B/\hbar) , \tag{1.6}$$

where the quantum-mechanical preexponential factor ω_q is related to the fluctuations about the bounce. The exponential factor smoothly matches onto the Arrhenius factor for $T=T_0$. While the Arrhenius factor is independent of damping, the bounce action is modified by dissipation leading to pronounced effects of friction in the quantum regime. Dissipation was first incorporated into the bounce technique for the calculation of tunneling rates by Caldeira and Leggett.[11] In our earlier work[5,6] and in independent studies by Larkin and Ovchinnikov,[12,13] the method was used as an effective scheme for the calculation of rates in the entire range of temperatures. In this paper we shall exclusively rely upon this method. Apart from the elegance of the approach, this choice is also dictated by the fact that at present there is no alternative method available for the calculation of quantum decay rates in the entire range of parameters of interest.

II. FREE ENERGY OF A DAMPED SYSTEM

In the absence of dissipation the coordinate representation of the canonical operator $\rho_\beta=\exp(-\beta H)$ of a particle of mass M moving in a potential $V(q)$ may be written[36]

$$\langle q' \mid \rho_\beta \mid q \rangle = \int D[q] \exp\left[-\frac{1}{\hbar}S[q]\right] , \tag{2.1}$$

where $\beta=1/k_B T$ is the inverse temperature, and where the functional integral is over all paths connecting $q(0)=q$ with $q(\hbar\beta)=q'$. The path probability is weighted according to the Euclidean action

$$S[q]=\int_0^{\hbar\beta} d\tau\left[\tfrac{1}{2}M\dot{q}^2+V(q)\right] . \tag{2.2}$$

Since the canonical operator may formally be considered as a time evolution operator $\exp(-iHt/\hbar)$ in imaginary time $t=-i\hbar\beta$, the integral (2.1) is frequently referred to as an imaginary time functional integral.

Naturally, environmental influences will modify the stationary density matrix of the particle. In the problem we wish to address the coupling to the environmental degrees of freedom is not of the most general form but such that the damping term in the classical deterministic equation of motion (1.1) is linear. A linear dissipative mechanism, however, can always be modeled by a heat bath consisting of an infinite set of harmonic oscillators. The system under study is then governed by the Lagrangian

$$L=\tfrac{1}{2}M\dot{q}^2-V(q)+\sum_i \tfrac{1}{2}m_i\left[\dot{q}_i^2-\omega_i^2\left[q_i-\frac{c_i}{m_i\omega_i^2}q\right]^2\right] . \tag{2.3}$$

Here the coupling term is written in a form that does not lead to a coupling induced renormalization of the potential.[11] The model characterized by (2.3) was studied frequently in the last two decades. Within a detailed realistic model of the environment, the model (2.3) is equivalent to an approximation where the response of the heat bath to the particle's motion is treated linearly. This corresponds to the assumption of linear damping. It should be noted that while each environmental degree of freedom is perturbed only weakly by the particle, the combined effect of these modes upon the particle's motion is not necessarily weak and can cause strong damping.

Investigating the classical dynamics generated by the Lagrangian (2.3), one finds that the deterministic equation of the motion of the particle is in fact of the form (1.1) with a damping kernel $\gamma(t)$ the Laplace transform of which is given in terms of the model parameters by[14,22]

$$\hat{\gamma}(z)=\int_0^\infty dt\,\gamma(t)\exp(-zt)=\frac{1}{M}\sum_i \frac{c_i^2}{m_i\omega_i^2}\frac{z}{z^2+\omega_i^2} . \tag{2.4}$$

A given phenomenological damping kernel can now easily be modeled by a suitable choice of the parameters in (2.3). On the other hand, the microscopic model can readily be quantized. In the imaginary time functional integral representation of the canonical operator of the entire system, the integrals over the environmental coordinates are Gaussian and they may be evaluated exactly.[36] Tracing over the heat-bath coordinates, one then arrives at a functional integral representation of the reduced equilibrium density matrix ρ_β of the damped particle which is again of the form (2.1), however, with an effective action[11,5]

$$S[q]=\int_0^{\hbar\beta} d\tau\left[\tfrac{1}{2}M\dot{q}^2+V(q)\right] + \tfrac{1}{2}\int_0^{\hbar\beta} d\tau \int_0^{\hbar\beta} d\tau' k(\tau-\tau')q(\tau)q(\tau') , \tag{2.5}$$

where the last term describes the influence of the environment. The influence kernel $k(\tau)$ is periodic with period $\hbar\beta$ and may be represented as a Fourier series

$$k(\tau)=\frac{1}{\hbar\beta}\sum_{n=-\infty}^{\infty}K(\nu_n)\exp(i\nu_n\tau)\ , \tag{2.6}$$

where the $\nu_n=2\pi n/\hbar\beta$ are the Matsubara frequencies. The Fourier coefficients are given in terms of the model parameters by

$$K(\nu_n)=\sum_i\frac{c_i^2}{m_i\omega_i^2}\frac{\nu_n^2}{\nu_n^2+\omega_i^2}\ . \tag{2.7}$$

Comparing (2.4) and (2.7) we see that $K(\nu_n)=M\,|\,\nu_n\,|\,\hat{\gamma}(\,|\,\nu_n\,|\,)$ which implies

$$k(\tau)=\frac{M}{\hbar\beta}\int_0^\infty ds\,\gamma(s)\frac{\partial}{\partial s}\frac{\sinh(\nu s)}{\cos(\nu\tau)-\cosh(\nu s)}$$
$$+M\gamma(0):\delta(\tau):\ , \tag{2.8}$$

where $\nu=\nu_1=2\pi/\hbar\beta$ and where $:\delta(\tau):$ is the δ function periodically repeated at $\tau=n\hbar\beta$, n integer. This equation connects the quantum-mechanical influence kernel $k(\tau)$ with the damping kernel $\gamma(t)$ of the classical equation of motion. Because of this relation further recourse to the microscopic model is not necessary. Note that the nonlocal form of the last term in (2.5) is not due to memory effects since $k(\tau)$ remains finite for finite τ even if $\gamma(t)$ decays infinitely fast (Ohmic damping).

The partition function Z_β of the damped particle is the trace over the equilibrium density matrix ρ_β. Using (2.1) we obtain

$$Z_\beta=\int D[q]\exp\left[-\frac{1}{\hbar}S[q]\right]\ , \tag{2.9}$$

where the functional integral is over all periodic paths with period $\hbar\beta$. The free energy is then given by

$$F=-\frac{1}{\beta}\ln Z_\beta\ . \tag{2.10}$$

By virtue of (2.5) and (2.8), the free energy is now specified completely in terms of quantities appearing in the classical equation of motion (1.1). This is the starting point for the further analysis.

III. THE CROSSOVER TEMPERATURE T_0

We shall be concerned here with a damped particle moving in a metastable well of the form depicted in Fig. 1. Thermal and quantum fluctuations let the particle escape from this well. Weak metastability requires a barrier height V_b which is large compared with other relevant energy scales, in particular

$$V_b\gg k_BT,\quad V_b\gg\hbar\omega_0\ . \tag{3.1}$$

Then, the functional integral (2.9) may be evaluated in a semiclassical approximation, i.e., the main contribution comes from the vicinity of those paths for which the action (2.5) is stationary. The extremal action paths satisfy the equation of motion

$$M\ddot{q}(\tau)-\frac{\partial V(q)}{\partial q(\tau)}-\int_0^{\hbar\beta}d\tau' k(\tau-\tau')q(\tau')=0 \tag{3.2}$$

and the boundary condition $q(0)=q(\hbar\beta)$. In the absence of dissipation the evolution equation (3.2) corresponds to a real time motion in the potential $-V(q)$. In this inverted potential (Fig. 2) there is a trivial periodic solution, $q(\tau)=0$, where the particle just sits on top of the potential barrier of the inverted potential, and another solution, $q(\tau)=q_b$, where it sits at the bottom of the well. However, for temperatures below $T_0=\hbar\omega_b/2\pi k_B$, the period $\hbar\beta=\hbar/k_BT$ is long enough to admit also an oscillation of the particle along a periodic orbit in the classically forbidden region. This latter trajectory is frequently called the bounce.

Since the influence kernel satisfies

$$\int_0^{\hbar\beta}d\tau\,k(\tau)=K(0)=0\ , \tag{3.3}$$

the trivial solutions $q(\tau)=0$ and $q(\tau)=q_b$ are not affected by dissipation although the action of paths in the vicinity of these trajectories is modified. The bounce, however, is changed by dissipation and exists in the damped case only for temperatures below the crossover temperature[5,6]

$$T_0=\hbar\omega_R/2\pi k_B\ . \tag{3.4}$$

where ω_R is the largest positive root of the equation

$$\omega_R^2+\omega_R\hat{\gamma}(\omega_R)=\omega_b^2\ . \tag{3.5}$$

It will become clear from below that T_0 is the temperature where roughly the transition between thermally activated decay and quantum tunneling occurs which is observed experimentally as a flattening of the rate as the temperature is lowered. This temperature is always reduced by dissipation which affects T_0 through the damping coefficient at frequency ω_R. For weak damping, ω_R is the order of the barrier frequency ω_b. In the particular case of Ohmic damping, $\hat{\gamma}(z)=\gamma$, we have

$$\omega_R=\omega_b[(1+\alpha^2)^{1/2}-\alpha] \tag{3.6}$$

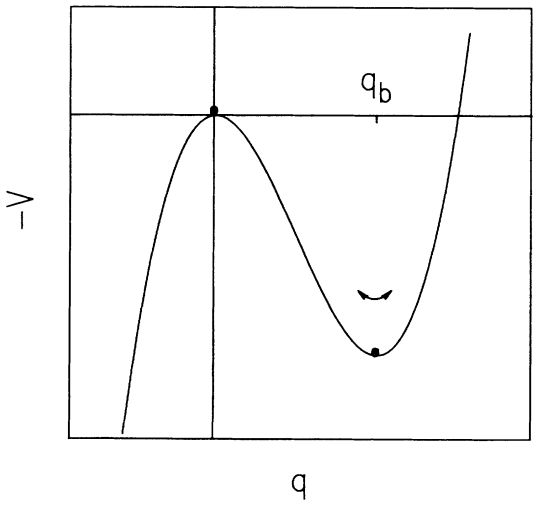

FIG. 2. The inverted potential $-V(q)$.

and hence[5]

$$T_0=(\hbar\omega_b/2\pi k_B)[(1+\alpha^2)^{1/2}-\alpha]\ , \tag{3.7}$$

where $\alpha=\gamma/2\omega_b$ is a dimensionless damping parameter.

In the escape problem, various temperature regions must be distinguished, in general (Fig. 3). Above T_0 the functional integral is dominated by the trivial semiclassical trajectories $q(\tau)=0$ and $q(\tau)=q_b$. The fluctuation modes about these trajectories lead to quantum corrections which become increasingly important as the crossover temperature is approached from above. The semiclassical approximation to the functional integral breaks down near T_0 where a new semiclassical trajectory, the bounce, emerges. This crossover region has to be treated with special care. Below T_0 the functional integral is dominated by the trivial solution $q(\tau)=0$ and the bounce $q_B(\tau)$. In this region quantum tunneling prevails. The calculation of the rate in various regions will be discussed in the following sections.

IV. THERMALLY ACTIVATED DECAY

In this section the thermodynamic method for the calculation of decay rates is utilized to determine the rate in the high-temperature region where thermal activation dominates. The calculation is carried out fully quantum mechanically and yields the quantum corrections to the familiar Arrhenius law.

A. Imaginary part of the free energy

For temperatures above T_0, the functional integral (2.9) may readily be evaluated in the semiclassical approximation where the main contribution arises from the vicinity of the time-independent trajectories $q(\tau)=0$ and $q(\tau)=q_b$. A periodic path near the stationary trajectory $q(\tau)=0$ may be written as

$$x(\tau)=\sum_{n=-\infty}^{\infty} X_n\exp(i\nu_n\tau)\ , \tag{4.1}$$

where again ν_n are the Matsubara frequencies. When (4.1) is inserted into (2.5) one finds for the action

$$S[x]=\tfrac{1}{2}M\hbar\beta\sum_{n=-\infty}^{\infty}\lambda_n^0 X_n X_{-n}\ , \tag{4.2}$$

where

$$\lambda_n^0=\nu_n^2+\omega_0^2+|\nu_n|\hat{\gamma}(|\nu_n|)\ , \tag{4.3}$$

and where terms of the third order in the amplitudes are disregarded. The contributions of these paths to the partition function (2.9) can now be determined by performing the Gaussian integrals over the amplitudes X_n. This gives the partition function Z_0 of a damped particle in a harmonic well.

A periodic path near the other stationary trajectory, $q(\tau)=q_b$, may be written as

$$y(\tau)=q_b+\sum_{n=-\infty}^{\infty} Y_n\exp(i\nu_n\tau)\ . \tag{4.4}$$

The second-order action now reads as

$$S[y]=\hbar\beta V_b+\tfrac{1}{2}M\hbar\beta\sum_{n=-\infty}^{\infty}\lambda_n^b Y_n Y_{-n}\ , \tag{4.5}$$

where

$$\lambda_n^b=\nu_n^2-\omega_b^2+|\nu_n|\hat{\gamma}(|\nu_n|)\ . \tag{4.6}$$

When we want to evaluate the contribution Z_b of these paths to the partition function we encounter a problem. Since the eigenvalue $\lambda_0^b=-\omega_b^2$ is negative, the trajectory $q(\tau)$ is not a minimum of the action but a saddle point with an unstable direction. Because of this negative mode, the integral over the amplitude Y_0 is divergent. This should come as not too big a surprise, after all we are trying to compute the free energy of an unstable system. Langer[31] has explained that in such a situation the functional integral can still be defined by distorting the integration contour into the upper half of the complex plane along the direction of the steepest descent which is the positive imaginary axis in the present case. This leads to an imaginary part of the partition function. When we write Z_β in the form $Z_\beta=Z_0(1+Z_b/Z_0)$ and note that, as a consequence of the first term in (4.5), the ratio Z_b/Z_0 contains the exponentially small factor $\exp(-\beta V_b)$, the associated imaginary part of the free energy is found to read

$$\begin{aligned}\mathrm{Im}F&=-(1/\beta Z_0)\mathrm{Im}Z_b\\&=-(1/2\beta)[D_0/|D_b|]^{1/2}\exp(-\beta V_b)\ .\end{aligned} \tag{4.7}$$

Here D_0 and D_b are the determinants connected with the second-order action functionals (4.2) and (4.5)

$$D_0=\prod_{n=-\infty}^{\infty}\lambda_n^0,\quad D_b=\prod_{n=-\infty}^{\infty}\lambda_n^b\ . \tag{4.8}$$

Note that the exponentially small contribution Z_b of the paths near $q(\tau)=q_b$ is kept in the semiclassical approximation of the functional integral (2.9) only because it gives not just a small correction to Z_0 but a contribution which is imaginary and hence of a different type.

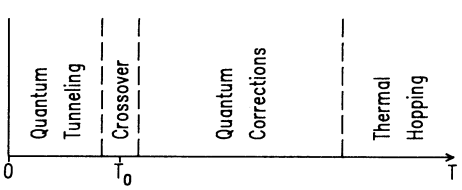

FIG. 3. The dominant escape mechanism is depicted schematically as a function of temperature.

B. The classical limit

Following Langer[31] the imaginary part of the free energy is now interpreted in the same way as the imaginary component of a resonance energy in quantum-field theory, namely, as a quantity describing the finite lifetime of the state. By analogy, we would define the decay rate through $\Gamma=-(2/\hbar)\mathrm{Im}F$. This is actually the formula which we shall use in the low-temperature region below

T_0. However, Affleck[32] has shown that above T_0 the rate has to be calculated by means of the modified formula $\Gamma=-(2/\hbar)(T_0/T)\mathrm{Im}F$. Hence, above T_0 there is an additional factor (T_0/T) as a remnant of the transition near T_0. Inserting (3.4) and (4.7) into the rate formula we obtain

$$\Gamma=\frac{\omega_0}{2\pi}\frac{\omega_R}{\omega_b}f_q\exp(-V_b/k_BT)\ , \tag{4.9}$$

where we made use of $\lambda_0^0=\omega_0^2$ and $\lambda_0^b=-\omega_b^2$, and where

$$f_q=\prod_{n=1}^{\infty}\frac{\lambda_n^0}{\lambda_n^b}=\prod_{n=1}^{\infty}\frac{\nu_n^2+\omega_0^2+\nu_n\hat{\gamma}(\nu_n)}{\nu_n^2-\omega_b^2+\nu_n\hat{\gamma}(\nu_n)} \tag{4.10}$$

contains the contribution of the remaining eigenvalues. As is apparent from the Arrhenius exponential factor, the rate (4.9) describes thermally activated transitions across the barrier. The factor f_q arises from quantum corrections and coincides with the result obtained by a different approach.[34] Because of $\nu_n=2\pi k_BTn/\hbar$, the factor f_q approaches unity for $T\gg T_0$. Hence, in the classical limit $k_BT\gg\hbar\omega_b$ the rate reduces to

$$\Gamma_{\mathrm{cl}}=\frac{\omega_0}{2\pi}\frac{\omega_R}{\omega_b}\exp(-V_b/k_BT)\ . \tag{4.11}$$

The factor ω_R/ω_b multiplying the transition-state preexponential factor $f_{\mathrm{TST}}=\omega_0/2\pi$ takes into account the effect of recrossings of the barrier top in the moderate to large friction region where the classical rate is limited by spatial diffusion across the barrier top. The classical rate formula (4.11) coincides with the results of earlier work[27] extending Kramers' approach to the case of memory friction. The frictional influence on the classical rate arises through the friction and memory renormalized barrier frequency ω_R. This frequency likewise appears in the expression (3.4) for the crossover temperature T_0. For frequency-independent damping the renormalized barrier frequency is given by (3.6) and one obtains from (4.11) the familiar Kramers result. Note that in the limit of vanishing friction the rate formula (4.11) reduces to the transition state result while the prefactor of the accurate rate decreases for low damping as a consequence of the nonequilibrium depletion effects in the metastable well. Hence, the proportionality between the rate and the imaginary part of the free energy does not extend to the region of energy diffusion limited classical escape occurring for extremely underdamped systems with $\hat{\gamma}(\omega_b)\lesssim\omega_bk_BT/V_b$.

C. Quantum corrections

As the temperature T is lowered, the classical escape rate (4.11) is modified by quantum corrections enhancing the decay probability. We have

$$\Gamma=f_q\Gamma_{\mathrm{cl}} \tag{4.12}$$

where f_q is the quantum correction factor (4.10). The leading quantum corrections have a rather simple origin. Quantum fluctuations facilitate the escape because they increase the average energy of the particle in the metastable well and, for a particle that is thermally excited almost up to the barrier top, they allow for tunneling through the remaining small barrier. Both effects lead to an effective reduction of the barrier. The resulting leading quantum corrections are found to be given by the simple formula[20]

$$f_q=\exp\left[\frac{\hbar^2}{24}(\omega_0^2+\omega_b^2)/(k_BT)^2\right]\ , \tag{4.13}$$

where terms of the order $(\hbar\omega_0/k_BT)^4$ were disregarded. Note that this high-temperature approximation of f_q holds independent of the dissipative mechanism. For frequency-independent damping the product (4.10) can be evaluated explicitly for all temperatures in terms of Γ functions yielding[34]

$$f_q=\frac{\Gamma(1-\lambda_b^+/\nu)\Gamma(1-\lambda_b^-/\nu)}{\Gamma(1-\lambda_0^+/\nu)\Gamma(1-\lambda_0^-/\nu)}\ , \tag{4.14}$$

where $\nu=2\pi k_BT/\hbar$ and where

$$\lambda_b^{\pm}=-\frac{\gamma}{2}\pm\left[\frac{\gamma^2}{4}+\omega_b^2\right]^{1/2},\quad \lambda_0^{\pm}=-\frac{\gamma}{2}\pm\left[\frac{\gamma^2}{4}-\omega_0^2\right]^{1/2}\ . \tag{4.15}$$

The temperature dependence of the factor f_q is depicted in Fig. 4.

For a strongly damped system $\gamma\gg\omega_0$, ω_b and $T\gg T_0$, the Ohmic quantum correction factor (4.14) can be simplified to read

$$f_q=\exp\left\{\frac{T_0}{T}\left[1+\frac{\omega_0^2}{\omega_b^2}\right]\left[\Psi\left[1+4\alpha^2\frac{T_0}{T}\right]-\Psi(1)\right]\right\}\ , \tag{4.16}$$

where $\Psi(x)$ is the digamma function and $\alpha=\gamma/2\omega_b$. For $T\gg4\alpha^2T_0$ this reduces to the high-temperature approxi-

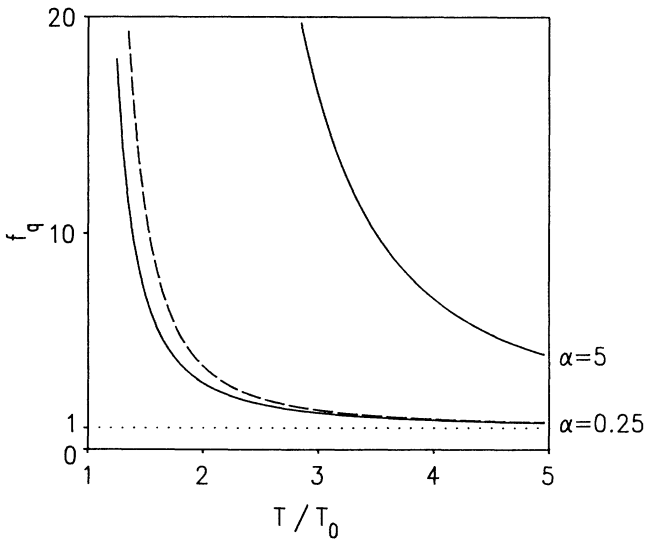

FIG. 4. The quantum correction factor f_q is shown as a function of temperature T for a system with $\omega_0=\omega_b$ and frequency independent damping for two values of $\alpha=\gamma/2\omega_b$. The dashed line shows the approximation (4.13) for the case $\alpha=0.25$.

mation (4.13). On the other hand, for intermediate temperatures $T_0 \ll T \ll 4\alpha^2 T_0$ one finds

$$f_q = (4\alpha^2 T_0/T)^{(1+\omega_0^2/\omega_b^2)T_0/T} . \tag{4.17}$$

Note that this factor can enhance the rate quite substantially even well above the crossover temperature.[37] For instance, for $T=4T_0$ and $\omega_0=\omega_b$, one finds $f_q \approx \alpha$.

For weakly damped systems where $\gamma \ll \omega_0$, ω_b one has approximately

$$f_q = \frac{\omega_b}{\omega_0} \frac{\sinh(\hbar\omega_0/2k_B T)}{\sin(\hbar\omega_b/2k_B T)} \exp[D\alpha + O(\alpha^2)] , \tag{4.18}$$

where

$$D = \frac{\omega_b}{\nu}[\Psi(1+\omega_b/\nu)+\Psi(1-\omega_b/\nu) - \Psi(1+i\omega_0/\nu)-\Psi(1-i\omega_0/\nu)] . \tag{4.19}$$

Naturally, the limit of small damping must be treated with care since for $\alpha < k_B T/V_b$, the rate is affected by nonequilibrium effects as discussed above. For weakly to moderately damped systems the quantum corrections are only essential for temperatures of a few T_0. Hence, as a function of T/T_0 the classical limit of the rate is approached more rapidly than for strongly damped systems.

Independent of the form of the damping, the quantum correction factor (4.10) becomes singular as T approaches the crossover temperature T_0. This hints at the breakdown of the semiclassical approximation for the functional integral (2.9), a problem which will be discussed in Sec. V.

V. THE CROSSOVER REGION

As we have seen in the preceding section, quantum corrections to the classical escape rate become increasingly important as the temperature is lowered and approaches the crossover temperature T_0. The semiclassical approximation of the imaginary time functional integral (2.9) used so far breaks down in the vicinity of T_0 because the eigenvalue $\lambda_1^b = \lambda_{-1}^b = \nu^2 - \omega_b^2 + \nu\hat{\gamma}(\nu)$ vanishes for $T=T_0$ so that the Gaussian integral over the amplitudes Y_1, Y_{-1} becomes divergent. Therefore, the functional integral over these fluctuation modes has to be evaluated beyond the Gaussian approximation. It is readily seen that the definition (3.4), (3.5) of the crossover temperature T_0 is just derived from the condition $\lambda_1^b(T_0)=0$.[6] Here we have tacitly assumed that the eigenvalue λ_1^b vanishes first as T is lowered which is the case for most models of the dissipative mechanism of interest. The vanishing eigenvalue points to the fact that below T_0 the evolution equation (3.2) admits a new oscillatory solution. As a consequence, the evaluation of the functional integral in the crossover region proceeds differently above and below T_0. Here we give an extended account of our previous study of the crossover region.[6] For $T > T_0$ an equivalent analysis was also given by Larkin and Ovchinnikov.[13]

A. Beyond steepest descent for $T > T_0$

To regularize the divergent integral we have to add terms of higher order in the amplitudes Y_1, Y_{-1} to the second-order action (4.5). Expanding the potential $V(q)$ about the barrier top

$$V(q) = V_b - \tfrac{1}{2}M\omega_b^2(q-q_b)^2 + \sum_{k=3}^{\infty} \frac{1}{k} M c_k (q-q_b)^k \tag{5.1}$$

one readily obtains from (2.5)

$$S[y] = \hbar\beta V_b + \tfrac{1}{2}M\hbar\beta \left[\sum_{n=-\infty}^{\infty} \lambda_n^b Y_n Y_{-n} + 2c_3(Y_{-2}Y_1^2 + Y_2 Y_{-1}^2 + 2Y_0 Y_1 Y_{-1}) + 3c_4 Y_1^2 Y_{-1}^2 \right] , \tag{5.2}$$

where terms up to the fourth order in Y_1, Y_{-1} were kept. For temperatures slightly above T_0, the contribution Z_b to the partition function can now be calculated by first integrating over the amplitudes Y_0 and $Y_{\pm n}$, $n \geq 2$ as before. Then, we are left with an integral over the amplitudes Y_1 and Y_{-1}. The integrand is determined by the effective action

$$\Delta S_1 = \tfrac{1}{2}M\beta(2\lambda_1^b Y_1 Y_{-1} + B Y_1^2 Y_{-1}^2) , \tag{5.3}$$

where

$$B = 4c_3^2/\omega_b^2 - 2c_3^2/\lambda_2^b + 3c_4 . \tag{5.4}$$

Using $2\pi^{-1/2}\int_z^\infty dt \exp(-z^2) = \mathrm{erfc}(z)$, the remaining integration is found to give the factor

$$1/\Lambda_1 = (\pi M\beta/2B)^{1/2} \mathrm{erfc}[\lambda_1^b (M\beta/2B)^{1/2}] \times \exp[(\lambda_1^b)^2 (M\beta/2B)] \tag{5.5}$$

which replaces the factor $1/\lambda_1^b$ obtained in the semiclassical approximation [cf. (4.10)]. Near T_0, λ_1^b may be written as

$$\lambda_1^b = -a\epsilon , \tag{5.6}$$

where $\epsilon = (T_0 - T)/T_0$ is negative above T_0 which is convenient for later purposes. The coefficient a is positive and reads

$$a = \omega_b^2 + \omega_R^2(1 + \partial\hat{\gamma}(\omega_R)/\partial\omega_R) . \tag{5.7}$$

The factor (5.5) thus takes the form

$$1/\Lambda_1 = \sqrt{\pi}(\kappa/a)\mathrm{erfc}(-\kappa\epsilon)\exp(\kappa^2\epsilon^2) , \tag{5.8}$$

where

$$\kappa = a(M\beta/2B)^{1/2} . \tag{5.9}$$

Clearly, $1/\Lambda_1$ remains finite in the limit $\epsilon \to 0$ and instead of (4.10) we now obtain for the quantum correction factor

$$f_q=(\lambda_1^0/\Lambda_1)f_R \ , \tag{5.10}$$

where

$$f_R=\prod_{n=2}^{\infty}(\lambda_n^0/\lambda_n^b) \tag{5.11}$$

is the regular part of the product (4.10). Hence, the singularity arising for $T\to T_0$ in the prefactor of the semiclassical rate formula (4.10) is removed by nonlinear terms in the action functional. Before entering a more detailed discussion of this result let us investigate the behavior of the rate for temperatures slightly below T_0.

B. Beyond steepest descent for $T<T_0$

For temperatures below T_0, a third extremal action path, namely the bounce, exists in addition to the two time-independent solutions $q(\tau)=0$ and $q(\tau)=q_b$ of the equation of motion (3.2). Since the bounce is a periodic trajectory, it may be written as a Fourier series

$$q_B(\tau)=q_b+\sum_{n=-\infty}^{\infty}Q_n\exp(i\nu_n\tau) \ . \tag{5.12}$$

Now, when $q_B(\tau)$ is an extremal action trajectory, $q_B(\tau+\tau_0)$ is also a solution of (3.2). Hence, there is in fact a whole family of bounces with different phases. We can choose a particular one by requiring $q_B(\tau)=q_B(-\tau)$ or, equivalently, $Q_n=Q_{-n}$. Clearly, a fluctuation about the bounce which leads to a mere phase shift will not change the action. The amplitudes Q_n are small near T_0 and they can be calculated perturbatively from (3.2). Using $\epsilon=(T_0-T)/T_0>0$ as a small parameter, one obtains the Q_n as a power series in $\sqrt{\epsilon}$.[6,12] The leading-order terms are

$$\begin{aligned} Q_1&=(a\epsilon/B)^{1/2} \ , \\ Q_0&=-(2c_3/\omega_b^2)Q_1^2 \ , \\ Q_2&=(c_3/\lambda_2^b)Q_1^2 \ , \end{aligned} \tag{5.13}$$

from which we obtain for the bounce action

$$S_B=\hbar\beta V_b-\tfrac{1}{2}\hbar\beta(Ma^2/B)\epsilon^2+O(\epsilon^3) \ . \tag{5.14}$$

Note that the bounce action is smaller than the action of the trivial saddle point $q(\tau)=q_b$. Hence, compared with this trivial solution the bounce trajectory $q_B(\tau)$ becomes more important as the temperature is lowered.

To study the fluctuation modes, we put $q(\tau)=q_B(\tau)+\xi(\tau)$ and expand $\xi(\tau)$ in a Fourier series

$$\xi(\tau)=\sum_{n=-\infty}^{\infty}\Xi_n\exp(i\nu_n\tau) \ . \tag{5.15}$$

The fluctuation $\xi(\tau)$ leads to a change of the action (2.5). Near T_0 we may insert the perturbative solution (5.13) of the bounce trajectory and the second-order action can be written as

$$S[q_B+\xi]=S_B+\tfrac{1}{2}M\hbar\beta\left[-\omega_b^2\hat{\Xi}_0^2+\sum_{n=3}^{\infty}2\lambda_n^b\Xi_n\Xi_{-n}+a\epsilon(\Xi_1+\Xi_{-1})^2\right]+2\lambda_2^b\hat{\Xi}_2\hat{\Xi}_{-2} \ , \tag{5.16}$$

where only terms of leading order in ϵ were kept and where we introduced the transformed amplitudes

$$\begin{aligned} \hat{\Xi}_0&=\Xi_0-(2c_3/\omega_b^2)(a\epsilon/B)^{1/2}(\Xi_1+\Xi_{-1}) \ , \\ \hat{\Xi}_{\pm2}&=\Xi_{\pm2}+(2c_3/\lambda_2^b)(a\epsilon/B)^{1/2}\Xi_{\pm1} \ . \end{aligned} \tag{5.17}$$

We see that a $\hat{\Xi}_0$ fluctuation leads to a decrease of the action so that the bounce is in fact a saddle point of the action. The main difference between the second-order action (4.5) above T_0 and the result (5.16) valid for temperatures slightly below T_0 is that the twofold degenerate eigenvalue $\lambda_1^b=\lambda_{-1}^b$ which would become negative below T_0 is now replaced by a small positive eigenvalue $\lambda_1=2a\epsilon$ and a vanishing eigenvalue $\lambda_{-1}=0$. As mentioned above, the zero mode is associated with a phase shift of the bounce. The corresponding eigenfunction has Fourier coefficients $\Xi_n\propto inQ_n/Q_1$. When such a fluctuation is inserted into the action one obtains no contribution of the considered order because of the form (5.13) of the Fourier coefficients of the bounce and the absence of a term proportional to $(\Xi_1-\Xi_{-1})^2$ in (5.16).

As a consequence of the small eigenvalues λ_1 and λ_{-1}, the amplitudes Ξ_1 and Ξ_{-1} of a fluctuation lead only to a small increase of the action (5.16). Hence, these amplitudes can become very large and the second-order approximation is again not sufficient. Rather, the action of a path $q(\tau)=q_B(\tau)+\xi(\tau)$ must be determined more accurately by taking into account terms of the third and fourth order in the amplitudes Ξ_1 and Ξ_{-1}. These higher-order terms include nonlinear couplings between the amplitudes Ξ_1,Ξ_{-1} and other Fourier coefficients. The relevant terms of this expansion read

$$\Delta S_{nl}=-M\hbar\beta[\,c_3(\Xi_2\Xi_{-1}^2+\Xi_{-2}\Xi_1^2+2\Xi_0\Xi_1\Xi_{-1})+3c_4Q_1(\Xi_1^2\Xi_{-1}+\Xi_{-1}\Xi_1^2)+\tfrac{3}{2}c_4\Xi_1^2\Xi_{-1}^2] \ . \tag{5.18}$$

Now (5.18) is added to (5.16) and this expression for the action is inserted into the functional integral (2.9) for the partition function. This way we can evaluate the contribution Z_B of trajectories in the vicinity of the bounce to the partition function.

The integrals over the stable modes ($\Xi_{\pm n}$, $n\geq2$) can be performed in semiclassical approximation. The integral over the negative mode (Ξ_0) can likewise be carried out by distorting the integration contour as above. This leads to an imaginary part of Z_B. One is left with an integral over the amplitudes Ξ_1 and Ξ_{-1} where the integrand is given in terms of the effective action[6]

$$\Delta S_1=\tfrac{1}{2}MB\hbar\beta[\,Q_1^2(\Xi_1+\Xi_{-1})^2+2Q_1(\Xi_1+\Xi_{-1})\Xi_1\Xi_{-1}+(\Xi_1\Xi_{-1})^2] \ . \tag{5.19}$$

Now, we introduce polar coordinates (ρ,ϕ) by $\rho\cos(\phi)=Q_1+\frac{1}{2}(\Xi_1+\Xi_{-1})$, $\rho\sin(\phi)=(1/2i)(\Xi_1-\Xi_{-1})$. Then, ΔS_1 turns out to be independent of ϕ. A change of ϕ just corresponds to a phase fluctuation of the bounce which does not change the action. After a corresponding transformation of the integration measure, the ϕ integral gives a factor of 2π. The ρ integral corresponds to an integration over the amplitude fluctuations of the bounce. These fluctuations can be as large as the bounce amplitude. In particular, trajectories with ρ near zero are in the vicinity of the trivial saddle point whose contribution cannot be separated from Z_B for small ϵ. The remaining ρ integral is of the form

$$I_\rho=\int_0^\infty d\rho\,\rho\exp\left[-\frac{\beta B}{2}(\tfrac{1}{2}\rho^2-Q_1^2)\right] \tag{5.20}$$

which may be transformed into an error integral. Finally, using $Z_\beta=Z_0(1+Z_B/Z_0)$ and (2.10), the imaginary part of the free energy emerges as

$$\mathrm{Im}F=-(1/2\beta)[D_0/\,|\,D_B''\,|\,]^{1/2}\sqrt{\pi}(\kappa/a)\times\mathrm{erfc}(-\kappa\epsilon)\exp(-S_B/\hbar)\ . \tag{5.21}$$

Here D_0 is the determinant (4.8) and

$$D_B''=\prod_{\substack{n=-\infty\\ n\neq\pm1}}^{\infty}\lambda_n^b \tag{5.22}$$

is the determinant connected with the second-order action functional (5.16) with the zero mode and the quasizero mode omitted.

The result (5.21) is valid for temperatures slightly below T_0. Now, inserting (5.13) and using $\Gamma=-(2/\hbar)\mathrm{Im}F$ one finds for the decay rate[6]

$$\Gamma=\frac{1}{\hbar\beta}\frac{\omega_0}{\omega_b}\frac{\lambda_1^0}{a}f_R\sqrt{\pi}\kappa\,\mathrm{erfc}(-\kappa\epsilon)\exp(\kappa^2\epsilon^2-V_b/k_BT)\ . \tag{5.23}$$

Since at the crossover temperature $1/\hbar\beta=\omega_R/2\pi$, the formula (5.23) coincides in fact with (4.9) when (5.10) is inserted there. Hence, (5.23) describes the behavior of the rate in the crossover region both above and below T_0.

C. The scaling region

For systems with high barriers and reasonably smooth potentials, the coefficient κ defined in (5.9) is much larger than 1. This follows from the fact that Ma^2/B is an energy of the order of the barrier height so that κ is of the order of $(V_b/\hbar\omega_R)^{1/2}\gg1$. The formula (5.23), which goes beyond the semiclassical approximation, is only needed in the region $|\kappa\epsilon|<1$, or

$$|T-T_0|\le T_0/\kappa\ , \tag{5.24}$$

where the argument of the erfc function is of order 1. Because of $\kappa\gg1$, the crossover region is narrow on the scale T_0. For temperatures above this region ($\kappa\epsilon<-1$) we can use

$$\sqrt{\pi}\kappa\,\mathrm{erfc}(-\kappa\epsilon)\exp(\kappa^2\epsilon^2)\simeq-1/\epsilon\quad\text{for }\kappa\epsilon<-1\ . \tag{5.25}$$

Hence, in view of $\lambda_1^b=-a\epsilon$, the formula (5.23) then reduces to the semiclassical rate (4.9), (4.10). For temperatures below the crossover region ($\kappa\epsilon>1$) we can use

$$\mathrm{erfc}(-\kappa\epsilon)\simeq2\quad\text{for }\kappa\epsilon>1 \tag{5.26}$$

and the rate (5.23) reduces to

$$\Gamma=[D_0/\,|\,D_B'\,|\,]^{1/2}(S_0/2\pi\hbar)^{1/2}\exp(-S_B/\hbar)\ , \tag{5.27}$$

where D_B' is the determinant connected with the second-order action functional (5.16) with the zero mode omitted while the quasi-zero-mode $\lambda_1=2a\epsilon$ is included. The remaining factors are lumped into

$$S_0=8\pi^2(Ma/B\hbar\beta)\epsilon\ . \tag{5.28}$$

The result (5.27) holds for $\kappa^{-1}<\epsilon\ll1$ and coincides in this region with the low-temperature semiclassical rate discussed below.

Within the crossover region (5.24) it is convenient to consider the quantity

$$y=\Gamma\exp(V_b/k_BT)\ . \tag{5.29}$$

In the classical limit this quantity is independent of T. However, quantum effects lead to an increase of y as T is lowered. Let us study y as a function of $x=T-T_0$. Then, we see from (5.23) that there is a temperature scale $x_0=T_0/\kappa$ and a frequency scale

$$y_0=\tfrac{1}{2}(\omega_0^2+\omega_b^2)\left[\frac{M\omega_R}{\hbar B}\right]^{1/2}\times\frac{\omega_0}{\omega_b}\prod_{n=2}^{\infty}\frac{n^2\omega_R^2+\omega_0^2+n\omega_R\hat{\gamma}(n\omega_R)}{n^2\omega_R^2-\omega_b^2+n\omega_R\hat{\gamma}(n\omega_R)} \tag{5.30}$$

so that

$$y/y_0=F(x/x_0)\ , \tag{5.31}$$

where $F(\xi)=\mathrm{erfc}(\xi)\exp(\xi^2)$ is a universal function which is independent of the form of the metastable potential and also independent of the dissipative mechanism (Fig. 5).[6] Only the scale factors x_0 and y_0 depend on the particular system under consideration. The rate follows the universal law (5.31) in the crossover region (5.24).

VI. QUANTUM TUNNELING

Below the crossover temperature T_0, the metastable state decays predominantly by quantum tunneling. The most probable escape path is the bounce trajectory $q_B(\tau)$ which for temperatures below the crossover region (5.24) has an action S_B that is substantially smaller than the action $\hbar\beta V_b$ of the trivial saddle-point trajectory $q(\tau)=q_b$. Hence, the contribution Z_b of the trivial saddle point to the partition function (2.9) may be disregarded and the imaginary part of the free energy arises predominantly from the contribution of paths in the vicinity of the bounce $q_B(\tau)$. This trajectory is an oscillatory solution of the nonlocal and nonlinear equation of motion (3.2). In this chapter we summarize the available analytical results deferring the numerical calculations required for a large region of the parameter space to the subsequent section.

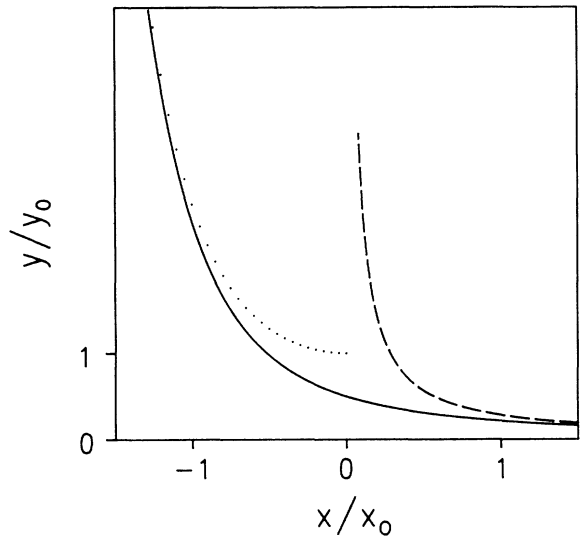

FIG. 5. The scaled rate y/y_0 is shown as a function of the scaled temperature x/x_0. The high-temperature formula (4.9) and (4.10) is shown as a dashed line and the low-temperature formula (5.27) as a dotted line. The crossover function smoothly matches onto these formulas valid outside the crossover region.

A. The quantum rate formula

Let us first derive the formal expression for the quantum decay rate in the semiclassical approximation. To evaluate the contribution of paths in the vicinity of the bounce to the partition function we proceed as earlier and expand the action (2.5) about the saddle-point trajectory. Putting $q(\tau)=q_B(\tau)+\xi(\tau)$ we find for the second-order action

$$S[q]=S_B+\int_0^{\hbar\beta}d\tau[\tfrac{1}{2}M\dot{\xi}^2+\tfrac{1}{2}V''(q_B(\tau))\xi^2] +\tfrac{1}{2}\int_0^{\hbar\beta}d\tau\int_0^{\hbar\beta}d\tau' k(\tau-\tau')\xi(\tau)\xi(\tau') , \quad (6.1)$$

where S_B is the action of the bounce trajectory. This may be written as

$$S[q]=S_B+\tfrac{1}{2}M\int_0^{\hbar\beta}d\tau\,\xi(\tau)L_B[\xi(\tau)] , \quad (6.2)$$

where

$$L_B[\xi(\tau)]=-\ddot{\xi}(\tau)+\frac{1}{M}V''(q_B(\tau))\xi(\tau) +\frac{1}{M}\int_0^{\hbar\beta}d\tau' k(\tau-\tau')\xi(\tau') \quad (6.3)$$

is a linear operator acting in the space of periodic functions with period $\hbar\beta$. The Gaussian functional integral over the fluctuations $\xi(\tau)$ may be expressed in terms of the eigenvalues of this operator. Now, differentiating the equation of motion (3.2) satisfied by $q_B(\tau)$ with respect to τ one finds

$$L_B[\dot{q}_B(\tau)]=0 . \quad (6.4)$$

Hence, $\dot{q}_B(\tau)$ is an eigenfunction of L_B with eigenvalue zero. This zero mode arises from the fact that the phase of the bounce is arbitrary. To linear order we have $q_B(\tau+\delta)=q_B(\tau)+\dot{q}_B(\tau)\delta$ which shows that the zero mode is in fact proportional to $\dot{q}_B(\tau)$. Since the bounce is periodic, the zero mode $\dot{q}_B(\tau)$ has one node within the interval $\hbar\beta$. By the node-counting theorem there exists a nodeless eigenmode of L_B with a smaller, negative eigenvalue. This negative eigenvalue points again to the fact that the system is unstable. The other eigenvalues of L_B are positive. The smallest positive eigenvalue, which merges into the quasi-zero-mode near T_0, is now sufficiently large so that all positive modes can be integrated out from the functional integral by steepest descents. The integration contour of the negative mode is distorted as above leading to an imaginary part of Z_B. The remaining integral over the zero mode is formally divergent. However, since the mode describes a shift of the bounce, this last integral sums over the family of bounces and it can be transformed explicitly into an integral over the bounce shift which varies over a finite interval.[35] From the change of the integration variable one picks up an additional factor which depends on the zero-mode normalization factor

$$S_0=M\int_0^{\hbar\beta}d\tau\,\dot{q}_B^2 . \quad (6.5)$$

This way the imaginary part of the ratio Z_B/Z_0 is obtained as

$$\mathrm{Im}Z_B/Z_0=\tfrac{1}{2}\hbar\beta(S_0/2\pi\hbar)^{1/2}[D_0/|D_B'|]^{1/2}\exp(-S_B/\hbar) , \quad (6.6)$$

where D_B' is the product of the eigenvalues of L_B with the zero eigenvalues omitted. Now, using[32] $\Gamma=-(2/\hbar)\mathrm{Im}F=(2/\hbar\beta)\mathrm{Im}Z_B/Z_0$ the quantum decay rate emerges as

$$\Gamma=\omega_q\exp(-S_B/\hbar) , \quad (6.7)$$

where

$$\omega_q=(S_0/2\pi\hbar)^{1/2}[D_0/|D_B'|]^{1/2} \quad (6.8)$$

is the quantum-mechanical prefactor of the rate while S_B is the bounce action. An analytical evaluation of this formula is generally only possible for temperatures near T_0 where the bounce can be calculated perturbatively. The action S_B is then given by (5.14) and the zero-mode factor (6.5) takes the form (5.28). Furthermore, for small $\epsilon=(T_0-T)/T_0$ the eigenvalues of L_B are found to read

$$\begin{aligned}&\lambda_0=-\omega_B^2+O(\epsilon) ,\\ &\lambda_1=2a\epsilon+O(\epsilon^2) ,\\ &\lambda_{-1}=0 ,\\ &\lambda_{\pm n}=\lambda_{\pm n}^b+O(\epsilon),\quad n\geq 2 ,\end{aligned} \quad (6.9)$$

which gives

$$D_B'=2a\epsilon\omega_b^2\left[\prod_{n=2}^{\infty}\lambda_n^b\right]^2 , \quad (6.10)$$

where again terms of order ϵ^2 were omitted. When these approximate expressions are inserted into the rate formula

(6.7) one finds

$$\Gamma=\frac{\omega_0}{\omega_b}\lambda_1^0\left[\prod_{n=2}^{\infty}\frac{\lambda_n^0}{\lambda_n^b}\right](\pi M/2\hbar^2\beta B)^{1/2}[1+O(\epsilon)]$$
$$\times\exp[-V_b/k_BT+\kappa^2\epsilon^2+O(\epsilon^3)] \tag{6.11}$$

which coincides with (5.23) for $\kappa\epsilon>1$ where $\mathrm{erfc}(-\kappa\epsilon)$ can be replaced by 2. Hence, the crossover formula (5.23) matches onto the semiclassical rate (6.7). In the region $\kappa^{-1}<\epsilon\ll 1$ the result (6.11) can be improved systematically by calculating higher-order terms in ϵ of the exponent and the prefactor. This is shown in Sec. VI C.

B. The case of a cubic potential and Ohmic damping

So far, we have considered arbitrary forms of the metastable potential and the general case of frequency-dependent damping. In the sequel however, we shall assume that the part of the potential relevant for the decay process can well be represented by a cubic

$$V(q)=\tfrac{1}{2}M\omega_0^2q^2(1-q/q_0)\ . \tag{6.12}$$

Here, q_0 is the tunneling length which is related to the barrier height through

$$V_b=2M\omega_0^2q_0^2/27\ . \tag{6.13}$$

Furthermore, we consider the case of frequency-independent or Ohmic damping characterized by the dimensionless parameter

$$\alpha=\gamma/2\omega_0\ . \tag{6.14}$$

Most of the analysis in the following sections can in fact be extended to the general case but some of the pertinent formulas become already quite lengthy in the special case discussed here.

The Fourier series (5.12) of the bounce trajectory may be rewritten as

$$q_B(\tau)=q_b+\tfrac{1}{3}q_0\sum_{n=-\infty}^{+\infty}R_n\exp(i\nu_n\tau)\ , \tag{6.15}$$

where the R_n are dimensionless Fourier coefficients. For Ohmic damping the Fourier representation (2.6) of the influence kernel is given by

$$k(\tau)=(M\gamma/\hbar\beta)\sum_{n=-\infty}^{+\infty}|\nu_n|\exp(i\nu_n\tau) \tag{6.16}$$

and the equation of motion (3.2) satisfied by the bounce may now be written as

$$2\mu_n^bR_n=\sum_{m=-\infty}^{+\infty}R_{n+m}R_{-m}\ , \tag{6.17}$$

where the dimensionless coefficients

$$\mu_n^b=n^2\Theta^2+2\alpha|n|\Theta-1 \tag{6.18}$$

are given as functions of the damping parameter α and the dimensionless temperature

$$\Theta=2\pi k_BT/\hbar\omega_0\ . \tag{6.19}$$

Again we choose a bounce trajectory with the symmetry $q_B(-\tau)=q_B(\tau)$ implying $R_{-n}=R_n$. Furthermore, introducing the dimensionless barrier height

$$v=V_b/\hbar\omega_0=2M\omega_0q_0^2/27\hbar \tag{6.20}$$

we may define a dimensionless bounce action

$$s=S_B/\hbar v \tag{6.21}$$

which by virtue of (6.15) and (6.17) may be expressed in terms of the Fourier coefficients as

$$s=(2\pi/\Theta)\left[1+\tfrac{1}{8}\sum_{n,m=-\infty}^{+\infty}R_{n+m}R_nR_m\right]\ . \tag{6.22}$$

Clearly, the dimensionless action s is only a function of the parameters α and Θ but independent of the barrier height. Furthermore, we introduce a dimensionless zero-mode normalization factor

$$g=S_0/2\pi\hbar v \tag{6.23}$$

which also is only a function of α and Θ. Using (6.5) and (6.15) we find

$$g=3\Theta\sum_{n=1}^{\infty}n^2R_n^2\ . \tag{6.24}$$

The expressions (6.22) and (6.24) are readily evaluated once a solution of (6.17) is found.

To study the eigenvalues of the fluctuation modes about the bounce trajectory we first note that the operator L_B introduced in (6.3) commutes with the parity operator $P[\xi(\tau)]=\xi(-\tau)$ provided we choose a bounce with the symmetry $q_B(\tau)=q_B(-\tau)$ as we have done above. Hence, the eigenfunctions of L_B are simultaneous eigenfunctions of the parity operator. Now, an eigenfunction with even parity is conveniently expanded as[38]

$$\xi(\tau)=q_0\Theta\left[Y_0+\sqrt{2}\sum_{n=1}^{\infty}Y_n\cos(\nu_n\tau)\right] \tag{6.25}$$

and the corresponding eigenvalue problem $L_B[\xi(\tau)]=\lambda\xi(\tau)=a\omega_0^2\xi(\tau)$ may be written as

$$\sum_{m=1}^{\infty}A_{n,m}Y_m=aY_n\ , \tag{6.26}$$

where a is the dimensionless eigenvalue and where the matrix coefficients $A_{n,m}$ are readily determined from (6.3) using the Fourier representations (6.15) and (6.16) of the bounce and the influence kernel as well as the form (6.12) of the potential. This yields[7]

$$\begin{aligned}A_{0,0}&=-(1+R_0)\ ,\\ A_{0,n}&=A_{n,0}=-\sqrt{2}R_n\ ,\\ A_{n,m}&=A_{m,n}=\mu_n^b\delta_{n,m}-(R_{n-m}+R_{n+m})\ ,\end{aligned} \tag{6.27}$$

where $n,m=1,2,\ldots$. Likewise, an eigenfunction with odd parity may be expanded as

$$\xi(\tau)=q_0\Theta\sqrt{2}\sum_{n=1}^{\infty}Z_n\sin(\nu_n\tau) \tag{6.28}$$

and the eigenvalue problem now takes the form

$$\sum_{m=1}^{\infty} B_{n,m} Z_m = b Z_n \ , \tag{6.29}$$

where b is again a dimensionless eigenvalue and where the matrix coefficients read[7]

$$B_{n,m} = B_{m,n} = \mu_n^b \delta_{n,m} - (R_{n-m} - R_{n+m}) \tag{6.30}$$

for $n,m = 1,2,\ldots$. The equations (6.26) and (6.29) are standard eigenvalue problems for real symmetric matrices. Hence, the matrices $A_{n,m}$ and $B_{n,m}$ have real eigenvalues a_n, $n = 0,1,2,\ldots$ and b_n, $n = 1,2,\ldots$, respectively. The eigenvalue a_0 is negative and b_1 is vanishing. The eigenfunctions associated with a_0 and b_1 are the unstable mode and the zero mode.

To proceed it is convenient to introduce a dimensionless prefactor χ which is related to the preexponential factor ω_q of the rate (6.7) by

$$\chi = 2\pi\omega_q / (\omega_0 \sqrt{v}\,) \ . \tag{6.31}$$

Using (6.8) this factor can be expressed in terms of the normalization factor (6.24) and the eigenvalues a_n and b_n of the matrices (6.27) and (6.30) as

$$\chi = 2\pi (g/|a_0|a_1)^{1/2} \mu_1^0 \prod_{n=2}^{\infty} \mu_n^0 (a_n b_n)^{-1/2} \ . \tag{6.32}$$

Here, the

$$\mu_n^0 = n^2\Theta^2 + 2\alpha |n| \Theta + 1 \tag{6.33}$$

are the dimensionless eigenvalues of the fluctuation modes about the metastable minimum for the case of Ohmic dissipation [cf. (4.3)]. By virtue of (6.21) and (6.31) the quantum rate formula (6.7) may now be cast into the form

$$\Gamma = \frac{\omega_0}{2\pi} \sqrt{v}\, \chi \exp(-vs) \tag{6.34}$$

in which the dependence upon the barrier height is shown explicitly since the dimensionless functions s and χ depend on α and Θ only.

At the end of this section we shortly summarize the results of the preceding sections specialized to a system with a cubic potential and Ohmic dissipation. The result (6.34) is valid for temperatures below the crossover region (5.24). In dimensionless units (6.19) the crossover temperature is given by

$$\Theta_0 = 2\pi k_B T_0 / \hbar\omega_0 = (\alpha^2+1)^{1/2} - \alpha \ . \tag{6.35}$$

The crossover region is now characterized by the condition

$$|\Theta_0 - \Theta| \le (rv)^{-1/2} \ , \tag{6.36}$$

where

$$r = 12\pi\Theta_0^{-1}(1+4\Theta_0^2)^{-1}(1+\alpha^2)(1+2\Theta_0^2) \ . \tag{6.37}$$

This condition can immediately be derived from (5.24) by virtue of (5.9) specified to the present case. In terms of the dimensionless quantities introduced in this section the decay rate (4.9) above the crossover region may be written as

$$\Gamma = \frac{\omega_0}{2\pi} \Theta_0 f_q \exp(-2\pi v/\Theta) \ , \tag{6.38}$$

where f_q is the quantum correction factor given by [cf. (4.14)]

$$f_q = \frac{\Gamma(1-\mu_b^+/\Theta)\Gamma(1-\mu_b^-/\Theta)}{\Gamma(1-\mu_0^+/\Theta)\Gamma(1-\mu_0^-/\Theta)} \tag{6.39}$$

with

$$\begin{aligned} \mu_b^{\pm} &= -\alpha \pm (\alpha^2+1)^{1/2} \ , \\ \mu_0^{\pm} &= -\alpha \pm (\alpha^2-1)^{1/2} \ . \end{aligned} \tag{6.40}$$

Now, since $\mu_b^+ = \Theta_0$, one of the Γ functions diverges as the crossover temperature Θ_0 is approached. Within the crossover region (6.36) we have to use the expression (5.23) for the decay rate. For Ohmic damping and a cubic potential, (5.23) gives

$$\Gamma = \frac{\omega_0}{2\pi} (\pi r v)^{1/2} \Theta_0^2 \frac{\Gamma(1-\mu_b^-/\Theta_0)}{\Gamma(1-\mu_0^+/\Theta_0)\Gamma(1-\mu_0^-/\Theta_0)} \operatorname{erfc}[(rv)^{1/2}(\Theta-\Theta_0)] \exp[-2\pi v/\Theta + rv(\Theta-\Theta_0)^2] \ . \tag{6.41}$$

This result smoothly interpolates between the high-temperature formula (6.38) and the low-temperature formula (6.34). Now all quantities which determine the temperature and damping dependence of the decay rate are explicitly known except for the dimensionless action s and the dimensionless prefactor χ in the quantum regime. The remainder of this paper will be concerned with the determination of these quantities as functions of α and θ.

Finally, we remark that both in the classical and the quantum regime the exponent of the rate is proportional to the barrier height v. However, while the classical exponent is independent of damping the quantum exponent strongly changes as a function of α. The high-temperature prefactor is independent of the barrier height except in the region of extremely small damping where the present theory does not apply. On the other hand, the quantum preexponential factor is proportional to $v^{1/2}$. The smooth matching between these prefactors occurs in the crossover region where the high-temperature prefactor follows roughly a $(\Theta-\Theta_0)^{-1}$ type singularity until it reaches values of order $v^{1/2}$ and is regularized by the erfc function in (6.41). Accordingly, the crossover region is of order $v^{-1/2}$ and hence very narrow in the semiclassical limit. In fact, the condition of weak metastability can be related to the condition that the crossover be narrow on the scale set by the crossover temperature, i.e.,

$$(rv)^{-1/2} \ll \Theta_0 \ . \tag{6.42}$$

For instance, requiring $(rv)^{-1/2}<0.1\Theta_0$, we find $V_b>5\hbar\omega_0$ for weakly damped systems ($\alpha\ll 1$) and $V_b>5\hbar\omega_0/\alpha$ for strongly damped systems ($\alpha\gg 1$). As a consequence, the barrier can be much lower when the system is heavily damped.

C. Expansion about the crossover temperature

In this section we shall calculate the exponent s of the quantum rate formula for temperatures near T_0 up to terms of third order in the expansion parameter

$$\epsilon=(T_0-T)/T_0=(\Theta_0-\Theta)/\Theta_0 \tag{6.43}$$

and the prefactor χ of the rate up to terms of first order in ϵ. We first note that in the equation of motion (6.17) satisfied by the bounce trajectory the temperature and damping dependence arises through the coefficients μ_n^b which in terms of ϵ may be written as

$$\mu_n^b=[n^2-2n(n-1)\alpha\Theta_0-1] -\epsilon 2n[n-(2n-1)\alpha\Theta_0]+\epsilon^2 n^2(1-2\alpha\Theta_0) . \tag{6.44}$$

This form immediately suggests a perturbative solution of (6.17) as a power series in $\epsilon^{1/2}$. It can be shown self-consistently that the coefficients R_n are of order $\epsilon^{(1+|n-1|)/2}$ when we seek for a solution with the symmetry $R_n=R_{-n}$. Hence, the perturbative solution of (6.17) is easily obtained by means of an iterative procedure. The largest Fourier coefficient is

$$R_1=(\epsilon K_0)^{1/2}[1+\tfrac{1}{2}\epsilon K_1+O(\epsilon^2)] , \tag{6.45}$$

where

$$K_0=4(1-\alpha\Theta_0)(3-4\alpha\Theta_0)/(5-8\alpha\Theta_0) \tag{6.46}$$

and

$$K_1=(5-8\alpha\Theta_0)^{-1}+(3-4\alpha\Theta_0)^{-1}+\tfrac{1}{2}(1-\alpha\Theta_0)^{-1} -K_0[\hat{\mu}_2^b+3(1-1/\hat{\mu}_3^b)/2\hat{\mu}_2^b]/(2\hat{\mu}_2^b-1) \tag{6.47}$$

in which

$$\hat{\mu}_n^b=n^2-2n(n-1)\alpha\Theta_0-1 \tag{6.48}$$

is the coefficient μ_n^b at the crossover temperature. The Fourier coefficients of the next two orders in $\epsilon^{1/2}$ are

$$R_0=-R_1^2-(R_1^4/2)[1+1/2(\hat{\mu}_2^b)^2] ,$$
$$R_2=R_1^2/2\mu_2^b+[R_1^4/2(\hat{\mu}_2^b)^2][(1/\hat{\mu}_0^b)+(1/\hat{\mu}_3^b)] , \tag{6.49}$$
$$R_3=R_1^3/2\hat{\mu}_2^b\hat{\mu}_3^b .$$

All higher Fourier coefficients are at least of order ϵ^2 and can be disregarded in the considered approximation. Now, from (6.22) we readily obtain for the dimensionless action

$$s=\frac{2\pi}{\Theta}-\frac{3\pi}{\Theta_0}K_0(1-\alpha\Theta_0)\epsilon^2[1+K_2\epsilon+O(\epsilon^2)] \tag{6.50}$$

where

$$K_2=\tfrac{2}{3}\alpha\Theta_0-\tfrac{17}{6}+(1-\alpha\Theta_0)^{-1} +(3-4\alpha\Theta_0)^{-1}+3(2-3\alpha\Theta_0)^{-1} +\tfrac{97}{12}(5-8\alpha\Theta_0)^{-1}+\tfrac{5}{4}(5-8\alpha\Theta_0)^{-2} . \tag{6.51}$$

Furthermore, the expansion of the dimensionless zero-mode normalization factor (6.24) is found as

$$g=3\Theta_0K_0\epsilon[1-K_3\epsilon+O(\epsilon^2)] \tag{6.52}$$

where

$$K_3=-\alpha\Theta_0+\tfrac{13}{4}+\tfrac{27}{8}(5-8\alpha\Theta_0)^{-1}-\tfrac{15}{8}(5-8\alpha\Theta_0)^{-2} -\tfrac{9}{2}(2-3\alpha\Theta_0)^{-1}-\tfrac{1}{2}(1-\alpha\Theta_0)^{-1} . \tag{6.53}$$

The relations (6.50) and (6.52) extend the results (5.14) and (5.28) to higher orders in ϵ for the case of a cubic potential with Ohmic damping.

Next we calculate the eigenvalues of fluctuations about the bounce for small ϵ. The matrices $A_{n,m}$ and $B_{n,m}$ introduced in (6.27) and (6.30) are already diagonal for $\epsilon=0$ so that the determination of their eigenvalues for small ϵ is a standard problem of perturbation theory. It is convenient to treat the terms proportional to the Fourier coefficients R_n as the perturbative part of the matrices $A_{n,m}$ and $B_{n,m}$. Then, the perturbation is at least of order $\epsilon^{1/2}$ and second-order perturbation theory is sufficient to calculate the eigenvalues up to terms of first order in ϵ. However, the eigenvalue a_1 which is itself of order ϵ, must be calculated up to terms of order ϵ^2 which means fourth-order perturbation theory. This way we find for $n>1$

$$a_n=\mu_n^b-(R_0+R_2)+\sum_{m=1}^{\infty}{}'(R_{n-m}+R_{n+m})^2/(\mu_n^b-\mu_m^b) +2R_n^2/(\mu_n^b-\mu_0^b)$$
$$=\mu_n^b+\epsilon K_0\{1-(2n\Theta_0^2+1)^{-1}+[2(n-1)\Theta_0^2+1]^{-1}\} , \tag{6.54}$$

where the second line follows by virtue of (6.44) and the expansions (6.45) and (6.49) of the Fourier coefficients R_n. Likewise, one obtains for $n>1$

$$b_n=a_n+O(\epsilon^2) . \tag{6.55}$$

The lowest eigenvalue b_1 of the matrix $B_{n,m}$ vanishes. The remaining eigenvalues are given by

$$a_0=-1-R_0+2\sum_{m=1}^{\infty}R_m^2/(\mu_0^b-\mu_m^b) \tag{6.56}$$

and

$$a_1=\mu_1^b+R_{11}+\sum_t{}'\frac{R_{1t}^2}{\mu_{1t}}+\sum_{s,t}{}'\frac{R_{1t}R_{ts}R_{s1}}{\mu_{1t}\mu_{1s}}-\sum_t{}'\frac{R_{11}R_{1t}^2}{\mu_{1t}^2}+\sum_{r,s,t}{}'\frac{R_{1r}R_{rs}R_{st}R_{t1}}{\mu_{1r}\mu_{1s}\mu_{1t}}$$
$$-2\sum_{s,t}{}'\frac{R_{11}R_{1s}R_{st}R_{t1}}{\mu_{1s}^2\mu_{1t}}-\sum_{s,t}{}'\frac{R_{1s}^2R_{1t}^2}{\mu_{1s}^2\mu_{1t}}+\sum_t{}'\frac{R_{11}^2R_{1t}^2}{\mu_{1t}^3}\ . \tag{6.57}$$

To write this result of fourth-order perturbation theory we introduced the abbreviations $\mu_{nm}=\mu_n^b-\mu_m^b$ and $R_{nm}=R_{n+m}+R_{n-m}$. After some algebra (6.57) yields

$$a_1=4(1-\alpha\Theta_0)\epsilon[1-K_3\epsilon+O(\epsilon^2)]\ , \tag{6.58}$$

where

$$K_3=-3\alpha\Theta_0+\tfrac{17}{4}-\tfrac{73}{8}(5-8\alpha\Theta_0)^{-1}+\tfrac{15}{8}(5-8\alpha\Theta_0)^{-2}$$
$$+\tfrac{9}{2}(2-3\alpha\Theta_0)^{-1}-\tfrac{1}{2}(1-\alpha\Theta_0)^{-1}-(3-4\alpha\Theta_0)^{-1}\ . \tag{6.59}$$

The above results may now be inserted into the expression (6.32) for the dimensionless quantum prefactor χ. The products arising in the intermediate results can be evaluated using the product representation of the Γ function. Since both the zero-mode factor g and the eigenvalue a_1 are proportional to ϵ, one factor of ϵ cancels in the expression (6.32). Therefore g and a_1 have to be inserted with accuracy ϵ^2 to obtain χ in order ϵ. The resulting expression for the prefactor reads as

$$\chi=\chi_0[1+B\epsilon+O(\epsilon^2)]\ , \tag{6.60}$$

where

$$\chi_0=4\pi\left[3\Theta_0\frac{3-4\alpha\Theta_0}{5-8\alpha\Theta_0}\right]^{1/2}$$
$$\times\Gamma(2-\hat{n}_b)/\Gamma(2-\hat{n}_0^+)\Gamma(2-\hat{n}_0^-) \tag{6.61}$$

and

$$B=5\alpha\Theta_0-\tfrac{29}{8}-\tfrac{51}{4}(5-8\alpha\Theta_0)^{-1}+\tfrac{15}{8}(5-8\alpha\Theta_0)^{-2}+\tfrac{9}{2}(2-3\alpha\Theta_0)^{-1}$$
$$+\tfrac{3}{2}(3-4\alpha\Theta_0)+\Psi(1)+\left[\frac{2\alpha}{\Theta_0}-1\right]\Psi\left[\frac{2\alpha}{\Theta_0}+1\right]+\hat{n}_0^+\Psi(2-\hat{n}_0^+)+\hat{n}_0^-\Psi(2-\hat{n}_0^-) \tag{6.62}$$

with

$$\hat{n}_b=[-\alpha-(\alpha^2+1)^{1/2}]/\Theta_0\ ,$$
$$\hat{n}_0^{\pm}=[-\alpha\pm(\alpha^2-1)^{1/2}]/\Theta_0\ .$$

The dependence of the quantities χ_0 and B on the damping strength α is shown in Fig. 6. Note that χ_0 is the prefactor of the semiclassical approximation to the quantum decay rate extrapolated to the crossover temperature. This must be distinguished from the true prefactor at T_0 since the semiclassical approximation is not valid in the vicinity of T_0. In fact, as is readily seen from (5.23) the true prefactor at the crossover temperature is $\chi_0/2$. This difference is also seen in Fig. 5, where both the semiclassical approximation and the rate in the crossover region are shown. The results of this section will be discussed further in connection with the numerical results presented in Sec. VII.

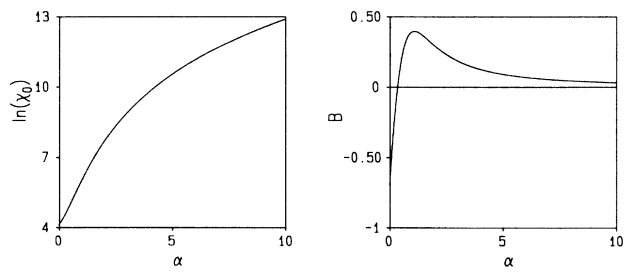

FIG. 6. The prefactor (6.61) and the logarithmic derivative (6.62) of the prefactor at the crossover temperature are shown as functions of α.

D. Expansion about zero temperature

For temperatures well below the crossover temperature analytical results on the parameter dependence of the exponent s and the prefactor χ are only known in limiting cases. The behavior of the quantum decay rate at zero temperature was studied in detail by Caldeira and Leggett.[11] Since they have given an extended presentation of their calculations we quote here only their results written in terms of the dimensionless quantities used above. For small damping they find for the zero-temperature action

$$\bar{s}=\frac{36}{5}\left[1+\frac{45\zeta(3)}{\pi^3}\alpha+O(\alpha^2)\right]\ , \tag{6.63}$$

where $\zeta(3)=1.202\ldots$ is a Riemann number. Here and in the sequel zero-temperature quantities are marked by an overbar. The prefactor is given by

$$\bar{\chi}=12\sqrt{6\pi}\ . \tag{6.64}$$

On the other hand, for very large damping one has

$$\bar{s}=6\pi\alpha\left[1+\frac{1}{4\alpha^2}+O(\alpha^{-4})\right] \tag{6.65}$$

and

$$\bar{\chi}=16\pi\sqrt{6}\alpha^{7/2}[1+O(\alpha^{-2}\ln\alpha)] , \tag{6.66}$$

where the latter result is due to Larkin and Ovchinnikov[13] who also showed that it remains valid up to Θ_0 for $\alpha \gg 1$. Recently, there have been attempts to determine the prefactor more precisely. For weak damping one has $\bar{\chi}=12\sqrt{6\pi}[1+c\alpha+\cdots]$, where Freidkin *et al.*[18] find $c=2.86$ while Ovchinnikov and Barone[23] obtain $c=4.076$. Our numerical results presented below indicate that the correct value is near $c=2.8$. On the other hand, for large damping the expansion of the prefactor reads[39] $\bar{\chi}=16\pi\sqrt{6}\alpha^{7/2}[1+2\alpha^{-2}\ln\alpha+d\alpha^{-2}+\cdots]$, where $d=\ln 2+\frac{1}{8}-\Psi(1)/2=1.107\ldots$.

At finite temperatures the tunneling rate is enhanced by thermal fluctuations. As was shown in a previous work,[5] the exponent of the rate follows a power law for low temperatures. The expansion of the bounce action about zero temperature was presented elsewhere[14] in detail for arbitrary forms of the metastable potential and arbitrary frequency dependence of the damping coefficient. Hence it is sufficient to give here only the result specified to the present problem. The expansion coefficients depend on the Fourier transform

$$q(\omega)=\frac{1}{2\pi}\int_{-\infty}^{+\infty} d\tau\, q_B(\tau)\exp(-i\omega\tau)=q_0\rho(\omega/\omega_0)/\omega_0 \tag{6.67}$$

of the zero-temperature bounce trajectory near $\omega=0$, where $\rho(\omega)$ is a dimensionless Fourier transform. For frequency-independent damping and a cubic potential one finds in terms of the dimensionless parameters introduced above

$$s=\bar{s}-\tfrac{9}{2}\pi\alpha\rho(0)^2[\Theta^2-\sigma\Theta^4+O(\Theta^6)] , \tag{6.68}$$

where $\bar{s}$ is the zero-temperature action and

$$\sigma=\frac{1}{10}\left[4\alpha^2-\frac{\rho''(0)}{\rho(0)}-5\alpha\left[\rho(0)-\alpha\frac{\partial\rho(0)}{\partial\alpha}\right]\right] . \tag{6.69}$$

The fourth-order term was obtained by extending our previous result.[14] The leading-order change of the action is proportional to Θ^2 and the associated numerical coefficient depends on $\rho(0)$ which is a dimensionless measure of the length of the zero-temperature bounce. Now, the Fourier transform $\rho(\omega)$ is not known for arbitrary strength of the damping. However, for vanishing damping one obtains from the equation of motion (2.5)

$$\rho(\omega)=2\omega/\sinh(\pi\omega) \tag{6.70}$$

and for strong damping, where the kinetic term may be disregarded, one has

$$\rho(\omega)=\tfrac{4}{3}\alpha\exp(-2\alpha|\omega|) . \tag{6.71}$$

Hence, combining (6.63) and (6.68) we obtain for small temperatures and weak damping

$$s=\frac{36}{5}\left[1+\frac{45\zeta(3)}{\pi^3}\alpha-\frac{5}{2\pi}\alpha\Theta^2-\frac{\pi}{12}\alpha\Theta^4+O(\alpha^2,\alpha\Theta^6)\right] \tag{6.72}$$

while combining (6.65) and (6.68), we find for low temperatures and strong damping

$$s=6\pi\alpha[1-\tfrac{4}{3}\alpha^2\Theta^2+O(\alpha^{-1})] . \tag{6.73}$$

It has been shown by Larkin and Ovchinnikov[13] that this high damping result remains valid up to the crossover temperature Θ_0 which for $\alpha \gg 1$ is given by $\Theta_0=1/2\alpha$. There is one further analytical result for an intermediate damping value chosen in such a way that a $\rho(\omega)$ of the form $\rho(\omega)=(a+b|\omega|)\exp(-c|\omega|)$ becomes an exact solution of the equation of motion. This way Riseborough *et al.*[17] find

$$\bar{s}=25.2 \quad \text{for } \alpha=1.175 . \tag{6.74}$$

For most regions of the (α,Θ) plane, analytical results are not available and the quantum decay rate has to be calculated by numerical methods which will be the subject of Sec. VII.

VII. NUMERICAL CALCULATION OF QUANTUM DECAY RATES

In this section we present the results of a numerical calculation of the exponent s and the prefactor χ of the quantum rate formula (6.34) covering a wide range of temperatures and damping coefficients namely, dimensionless temperatures between $\Theta=0.1\Theta_0$ and $\Theta=0.95\Theta_0$ and damping parameters between $\alpha=0$ and $\alpha=10$. This basically exhausts the parameter space since for temperatures below $0.1\Theta_0$ the changes of s and χ are below 1%, and for Θ near Θ_0 the rate matches onto the analytical result given in Sec. VI C. Furthermore for $\alpha=10$ the numerical results agree already with the asymptotic analytical results for large α within an accuracy of 1% for s and 4% for χ. The present work extends a calculation by Chang and Chakravarty[15] aiming at a determination of the zero-temperature rate. However, the discretization used by these authors introduces an effective temperature which is of the order of the lowest temperature explored here. In fact, our results for $\Theta/\Theta_0=0.1$ are in good agreement with those of Chang and Chakravarty[15] except for some differences in the prefactors for high damping where our calculations are more precise. Parts of our finite-temperature results were already given elsewhere.[7]

A. The bounce action

The calculation of the exponent of the rate starts out from the equation of motion (6.17) for the bounce which in view of $R_n=R_{-n}$ may also be written as

$$(n^2\Theta^2+2\alpha n\Theta-1)R_n=2\sum_{m=1}^{\infty}R_{n+m}R_m+\sum_{m=1}^{n}R_{n-m}R_m . \tag{7.1}$$

A numerical solution of this equation can easily be obtained by successive iterations starting for instance with a zeroth-order approximation of the form $R_n\propto\exp(-n)$. However, as already noted by Chang and Chakravarty,[15] a straightforward iteration of (7.1) drives the solution either to zero or infinity because of an unstable direction of

the iteration. This difficulty is avoided by solving the stable iteration

$$(n^2\Theta^2+2\alpha n\Theta-1)R'_n = (1/R'_0)^2\left[2\sum_{m=1}^{\infty}R'_{n+m}R'_m+\sum_{m=1}^{n}R'_{n-m}R'_m\right] \quad (7.2)$$

the solution of which immediately yields a solution

$$R_n = R'_n/R'^2_0 \quad (7.3)$$

of the problem (7.1). The coefficients R_n rapidly decay for larger n. The largest vectors are needed for $\alpha=10$ and $\Theta/\Theta_0=0.1$ where the sum in (7.2) can be truncated at $N=500$. No change of the results was observed for larger N. In the entire range of parameters the iteration converges within less than 100 steps except for Θ between $0.99\Theta_0$ and Θ_0. Since near Θ_0 the rate is known analytically, this latter region was not explored numerically.

By virtue of (6.22) and (6.24) the dimensionless bounce action s and the zero-mode factor g are simple sums over the Fourier coefficients R_n. The numerical values for these quantities obtained from the iterative solution of (7.1) have a relative error of less than 0.1%. Sample numerical results for s are summarized in Table I. The value for $\Theta=\Theta_0$ is supplemented using (6.50). The results for g are not given explicitly here but are needed for the calculation of the prefactor χ discussed in the following section. The temperature dependence of the action is also shown in Fig. 7 for three different values of α. The numerical values are compared with the analytical result (6.50) for high temperatures and with the Θ^2 approximation for the low-temperature action. For this purpose we have retained the first two terms of (6.68) and used the approximation

$$\rho(0)=\frac{1}{\pi}\{[4+(3-4\pi/3)^2\alpha^2]^{1/2}+3\alpha\} \quad (7.4)$$

for the bounce length which is a very good interpolation between the low damping value $\rho(0)=(2+3\alpha)/\pi$ and the high damping value $\rho(0)=4\alpha/3$. Clearly, the action follows the Θ^2 law very accurately up to quite high temperatures. For instance, for $\Theta=0.5\Theta_0$ the deviations of the first two terms of (6.68) from the correct numerical value are less than 0.5 percent for all damping values. For high damping the Θ^2 law holds for all temperatures up to Θ_0. Furthermore, the numerical values for s agree with the expansion (6.50) about the crossover temperature down to $\Theta=0.8\Theta_0$ with an accuracy of 1% and approach the analytical result for $\Theta\to\Theta_0$.

B. Eigenvalues and the preexponential factor

To determine the preexponential factor of the quantum decay rate we have to determine the eigenvalues a_n and b_n of the matrices $A_{n,m}$ and $B_{n,m}$ introduced in (6.27) and (6.30). Since the Fourier coefficients R_n decay for large n, the eigenvalues a_n and b_n approach μ_n^b in this limit. Hence, the large eigenvalues can be calculated perturbatively. Second-order perturbation theory gives

$$\begin{aligned} a_n &= \mu_n^b - 3\Theta(R_0+R_{2n}) \\ &\quad +9\Theta^2\sum_{m=0}^{\infty}{}'(\mu_n^b-\mu_m^b)^{-1}(R_{n-m}+R_{n+m})^2 , \\ b_n &= \mu_n^b - 3\Theta(R_0-R_{2n}) \\ &\quad +9\Theta^2\sum_{m=1}^{\infty}{}'(\mu_n^b-\mu_m^b)^{-1}(R_{n-m}-R_{n+m})^2 , \end{aligned} \quad (7.5)$$

where $\sum'$ means, as usual, the sum over all values except

TABLE I. Data of the exponent s of the decay rate as function of Θ/Θ_0 and α.

	Θ/Θ_0										
α	0.1	0.2	0.3	0.4	0.5	0.6	0.7	0.8	0.9	0.95	1.0
0.00	7.20	7.20	7.20	7.20	7.20	7.19	7.14	7.03	6.77	6.56	6.28
0.05	7.83	7.83	7.81	7.79	7.75	7.70	7.61	7.44	7.13	6.90	6.61
0.10	8.49	8.47	8.44	8.39	8.32	8.23	8.09	7.87	7.51	7.26	6.94
0.15	9.15	9.13	9.08	9.01	8.91	8.78	8.59	8.31	7.90	7.63	7.30
0.20	9.84	9.80	9.73	9.64	9.51	9.34	9.10	8.78	8.31	8.02	7.66
0.25	10.5	10.5	10.4	10.3	10.1	9.91	9.63	9.25	8.74	8.42	8.05
0.30	11.2	11.2	11.1	10.9	10.7	10.5	10.2	9.74	9.18	8.84	8.44
0.40	12.7	12.6	12.5	12.3	12.0	11.7	11.3	10.8	10.1	9.72	9.28
0.50	14.2	14.1	13.9	13.7	13.4	13.0	12.5	11.8	11.1	10.7	10.2
0.60	15.8	15.6	15.4	15.1	14.7	14.3	13.7	13.0	12.1	11.6	11.1
0.80	18.9	18.8	18.5	18.1	17.6	17.0	16.2	15.3	14.3	13.7	13.1
1.00	22.2	22.0	21.7	21.2	20.6	19.8	18.9	17.8	16.6	15.9	15.2
2.00	39.7	39.3	38.6	37.7	36.5	35.1	33.4	31.4	29.1	27.9	26.6
3.00	57.8	57.3	56.3	55.0	53.2	51.1	48.6	45.7	42.4	40.6	38.7
4.00	76.3	75.5	74.2	72.5	70.2	67.4	64.0	60.2	55.9	53.5	51.0
5.00	94.9	93.9	92.3	90.1	87.2	83.8	79.6	74.9	69.5	66.5	63.5
6.00	113.0	112.0	110.0	108.0	104.0	100.0	95.3	89.6	83.1	79.6	75.9
7.00	132.0	131.0	129.0	126.0	122.0	117.0	111.0	104.0	96.8	92.7	88.4
8.00	151.0	149.0	147.0	143.0	139.0	133.0	127.0	119.0	111.0	106.0	101.0
9.00	170.0	168.0	165.0	161.0	156.0	150.0	142.0	134.0	124.0	119.0	113.0
10.00	188.0	186.0	183.0	179.0	173.0	166.0	158.0	149.0	138.0	132.0	126.0

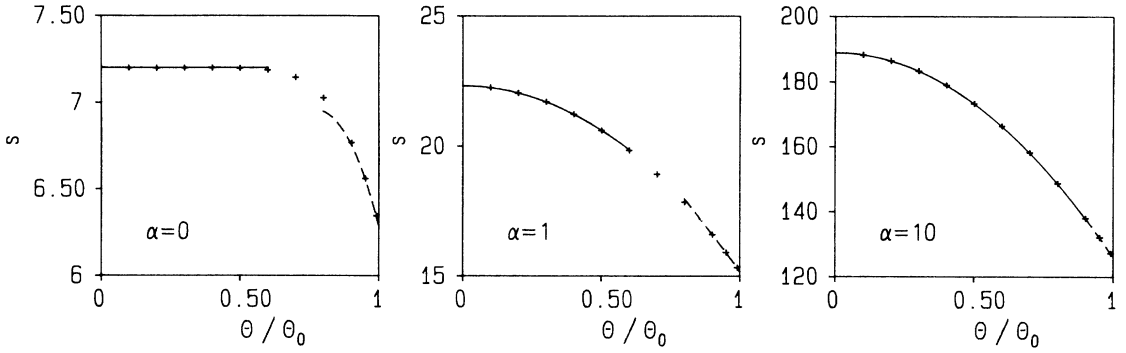

FIG. 7. The action as a function of temperature is shown for three different values of α. The solid and dashed lines show low- and high-temperature approximations (see text).

$n=m$. For small n the eigenvalues a_n and b_n can be calculated numerically by diagonalizing truncated $N\times N$ matrices $A_{n,m}$ and $B_{n,m}$. We have chosen N so that at least ten consecutive eigenvalues coincide with the perturbative result (7.5) with an error less than 10^{-6}. In the parameter range explored the largest N needed was $N=250$. Because of the effect of finite matrix size, the agreement between the numerical diagonalization and (7.5) is best for $n=n_c$, which is a few tens below N. The two methods to calculate the eigenvalues have been matched at $n=n_c$. The temperature dependence of the lowest eigenvalues is shown in Fig. 8.

The numerical results can now be inserted into the formula (6.32) for the prefactor χ. The infinite product is split into three factors. To evaluate the product from $n=2$ to $n=n_c$ we use the eigenvalues from the numerical diagonalization. These are about 200 factors each of which has a relative error well below 10^{-5} so that this part of the product has an error smaller than 10^{-3}. For very large n the eigenvalues are given by

$$a_n=b_n=\mu_n^b-3\Theta R_0\ . \tag{7.6}$$

Since with this approximation the infinite product can be expressed in terms of gamma functions, we can determine a cutoff n_b such that the infinite product from $n=n_b$ to $n=\infty$ gives a factor of 1 within a relative error of 10^{-3}. This yields a cutoff n_b between 10^4 and 10^6 depending on α and Θ. For the remaining product between $n=n_c+1$ and $n=n_b$ the eigenvalues are determined from (7.5) in double precision (15 digits) assuring that despite the large number of factors the relative error of the product is again below 10^{-3}. Since the zero-mode factor g is calculated with an error of less than 10^{-3} by the method explained in the preceding section, we obtain numerical results for the prefactor (6.32) with an estimated error of about 0.1%. Sample numerical results are summarized in Table II. Again the extrapolated value to $\Theta=\Theta_0$ is supplemented using the analytic result (6.61). Table II shows that below Θ_0 the temperature dependence of the prefactor is rather weak. As a consequence, the change of the prefactor in the quantum regime is hardly noticeable when the decay rate is depicted on a logarithmic scale as it is widely done. Figure 9 shows the quantum prefactor as a function of Θ/Θ_0 for three different values of the damping and compares the numerical values with the analytical result (6.60) valid near Θ_0. Note the different scale of the ordinates, which, for instance, blows up the change of 1.5% of the prefactor for $\alpha=10$ between $\Theta=0$ and $\Theta=\Theta_0$. This completes the numerical calculation of the rate in the quantum regime. Within the accuracy of the numerical calculation the results agree with the available analytical results discussed in Sec. VI.

VIII. CONCLUSIONS

The imaginary-time functional-integral approach to reaction rates which we have presented here has provided a

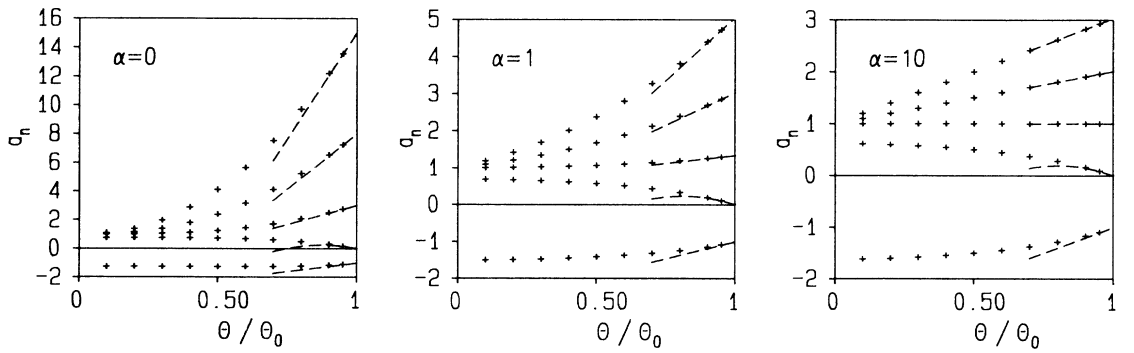

FIG. 8. The eigenvalues $a_0,\ldots,a_4$ are shown as functions of Θ for different values of α. The dashed lines show the analytical results for temperatures near Θ_0 derived in Sec. VI C.

TABLE II. Data of the prefactor χ of the decay rate as function of Θ/Θ_0 and α.

	Θ/Θ_0										
α	0.1	0.2	0.3	0.4	0.5	0.6	0.7	0.8	0.9	0.95	1.0
0.00	5.21×10^{1}	5.21×10^{1}	5.21×10^{1}	5.21×10^{1}	5.22×10^{1}	5.25×10^{1}	5.35×10^{1}	5.53×10^{1}	5.81×10^{1}	6.00×10^{1}	6.20×10^{1}
0.05	6.00×10^{1}	5.99×10^{1}	5.97×10^{1}	5.94×10^{1}	5.92×10^{1}	5.92×10^{1}	5.97×10^{1}	6.11×10^{1}	6.34×10^{1}	6.50×10^{1}	6.68×10^{1}
0.10	6.88×10^{1}	6.86×10^{1}	6.82×10^{1}	6.77×10^{1}	6.71×10^{1}	6.67×10^{1}	6.68×10^{1}	6.76×10^{1}	6.94×10^{1}	7.08×10^{1}	7.22×10^{1}
0.15	7.87×10^{1}	7.83×10^{1}	7.78×10^{1}	7.70×10^{1}	7.60×10^{1}	7.52×10^{1}	7.47×10^{1}	7.50×10^{1}	7.62×10^{1}	7.73×10^{1}	7.85×10^{1}
0.20	8.98×10^{1}	8.93×10^{1}	8.84×10^{1}	8.73×10^{1}	8.60×10^{1}	8.46×10^{1}	8.37×10^{1}	8.34×10^{1}	8.40×10^{1}	8.46×10^{1}	8.56×10^{1}
0.25	1.02×10^{2}	1.01×10^{2}	1.00×10^{2}	9.89×10^{1}	9.71×10^{1}	9.53×10^{1}	9.37×10^{1}	9.28×10^{1}	9.27×10^{1}	9.31×10^{1}	9.36×10^{1}
0.30	1.16×10^{2}	1.15×10^{2}	1.14×10^{2}	1.12×10^{2}	1.10×10^{2}	1.07×10^{2}	1.05×10^{2}	1.03×10^{2}	1.03×10^{2}	1.03×10^{2}	1.03×10^{2}
0.40	1.48×10^{2}	1.47×10^{2}	1.45×10^{2}	1.42×10^{2}	1.39×10^{2}	1.35×10^{2}	1.32×10^{2}	1.28×10^{2}	1.26×10^{2}	1.25×10^{2}	1.25×10^{2}
0.50	1.87×10^{2}	1.85×10^{2}	1.83×10^{2}	1.79×10^{2}	1.75×10^{2}	1.70×10^{2}	1.65×10^{2}	1.60×10^{2}	1.56×10^{2}	1.54×10^{2}	1.52×10^{2}
0.60	2.34×10^{2}	2.32×10^{2}	2.29×10^{2}	2.24×10^{2}	2.19×10^{2}	2.12×10^{2}	2.05×10^{2}	1.99×10^{2}	1.92×10^{2}	1.89×10^{2}	1.87×10^{2}
0.80	3.57×10^{2}	3.54×10^{2}	3.50×10^{2}	3.43×10^{2}	3.34×10^{2}	3.25×10^{2}	3.14×10^{2}	3.03×10^{2}	2.92×10^{2}	2.86×10^{2}	2.81×10^{2}
1.00	5.29×10^{2}	5.25×10^{2}	5.18×10^{2}	5.09×10^{2}	4.97×10^{2}	4.84×10^{2}	4.68×10^{2}	4.52×10^{2}	4.35×10^{2}	4.27×10^{2}	4.18×10^{2}
2.00	2.57×10^{3}	2.55×10^{3}	2.54×10^{3}	2.51×10^{3}	2.48×10^{3}	2.44×10^{3}	2.39×10^{3}	2.34×10^{3}	2.28×10^{3}	2.25×10^{3}	2.22×10^{3}
3.00	8.08×10^{3}	8.06×10^{3}	8.02×10^{3}	7.97×10^{3}	7.91×10^{3}	7.83×10^{3}	7.74×10^{3}	7.63×10^{3}	7.52×10^{3}	7.45×10^{3}	7.38×10^{3}
4.00	1.96×10^{4}	1.96×10^{4}	1.95×10^{4}	1.94×10^{4}	1.93×10^{4}	1.92×10^{4}	1.90×10^{4}	1.89×10^{4}	1.87×10^{4}	1.86×10^{4}	1.84×10^{4}
5.00	4.01×10^{4}	4.00×10^{4}	4.00×10^{4}	3.98×10^{4}	3.97×10^{4}	3.95×10^{4}	3.93×10^{4}	3.90×10^{4}	3.87×10^{4}	3.86×10^{4}	3.84×10^{4}
6.00	7.30×10^{4}	7.29×10^{4}	7.28×10^{4}	7.26×10^{4}	7.24×10^{4}	7.21×10^{4}	7.18×10^{4}	7.15×10^{4}	7.11×10^{4}	7.09×10^{4}	7.06×10^{4}
7.00	1.22×10^{5}	1.22×10^{5}	1.22×10^{5}	1.22×10^{5}	1.21×10^{5}	1.21×10^{5}	1.21×10^{5}	1.20×10^{5}	1.20×10^{5}	1.19×10^{5}	1.19×10^{5}
8.00	1.91×10^{5}	1.91×10^{5}	1.91×10^{5}	1.91×10^{5}	1.90×10^{5}	1.90×10^{5}	1.89×10^{5}	1.89×10^{5}	1.88×10^{5}	1.88×10^{5}	1.87×10^{5}
9.00	2.85×10^{5}	2.85×10^{5}	2.85×10^{5}	2.85×10^{5}	2.84×10^{5}	2.84×10^{5}	2.83×10^{5}	2.82×10^{5}	2.81×10^{5}	2.81×10^{5}	2.80×10^{5}
10.00	4.09×10^{5}	4.09×10^{5}	4.08×10^{5}	4.08×10^{5}	4.07×10^{5}	4.07×10^{5}	4.06×10^{5}	4.05×10^{5}	4.04×10^{5}	4.03×10^{5}	4.03×10^{5}

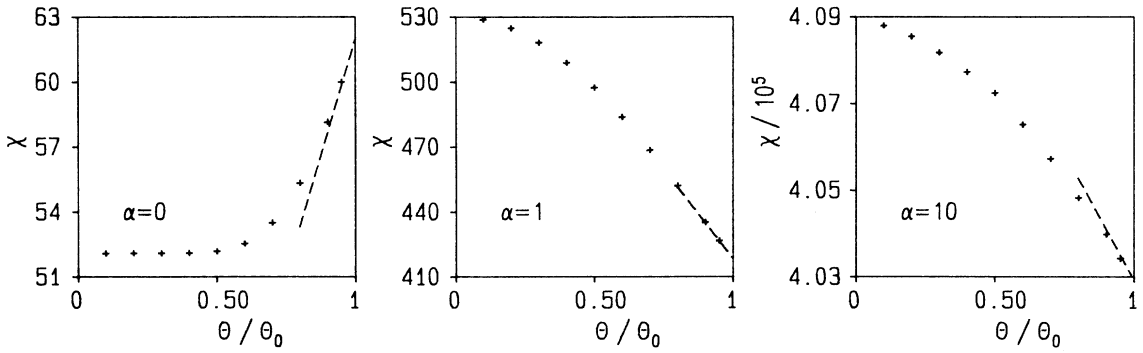

FIG. 9. The temperature dependence of the quantum prefactor is shown for three different values of α.

complete description of the quantum statistical decay of a metastable state extending from the classical regime where the rate follows an Arrhenius law down to very low temperatures where the system tunnels from its ground state. The main features of our results are summarized in the Arrhenius plot shown in Fig. 10. In this rate diagram the classical result is represented by a falling straight line. Because of quantum effects the rate does not decrease with a constant slope as T is lowered but flattens off towards a finite value at $T=0$. For an undamped system ($\alpha=0$) the transition between the classical and the quantum regime is rather sharp. In the presence of damping the classical rate is reduced only slightly because the attempt frequency is diminished by the factor ω_R/ω_b. On the other hand, damping causes an exponentially strong suppression of the zero-temperature tunneling rate. Furthermore, the crossover temperature is lowered and the transition between thermally activated and tunneling processes becomes more gradual for strong damping. For a damped system there is a large region where thermal and quantum fluctuations interplay. The low-temperature behavior of the rate is now governed by the power law (6.68) which dominates the rate since the preexponential factor depends only weakly on T. The range of validity of this behavior is shown in Fig. 11.

The theory presented here is applicable to the phenomenon of macroscopic quantum tunneling in Josephson devices.[2–4,8,9] These systems can be fabricated for a range of parameters so that they allow for a systematic study of the parameter dependence of the rate. Many of the theoretical predictions have indeed been confirmed by recent experiments.[3,40] This application will be discussed in greater detail elsewhere.

The interplay between thermal and quantum fluctuations is also observed in many molecular processes in physical and chemical systems.[29] Often a little *a priori* information about the potential shape and the environmental coupling is available and one hopes to extract this information from the parameter dependence of the measured rate. In this context it is important to be aware of the approximations inherent in a given rate formula.

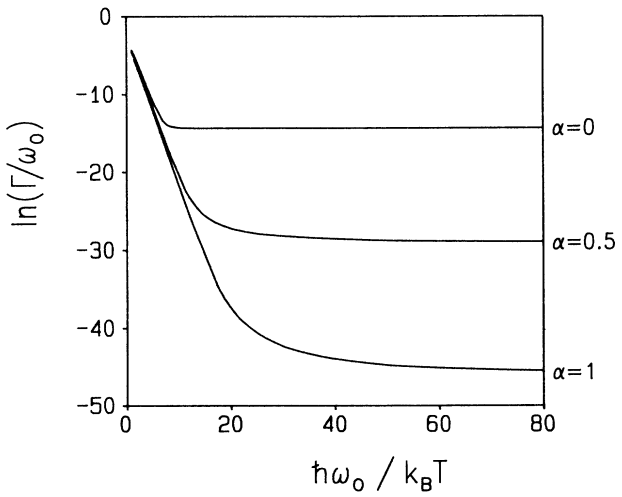

FIG. 10. Arrhenius plot of the decay rate for a system with a cubic potential ($V_b=5\hbar\omega_0$) and frequency-independent damping $\gamma=2\omega_0\alpha$ for various values of α.

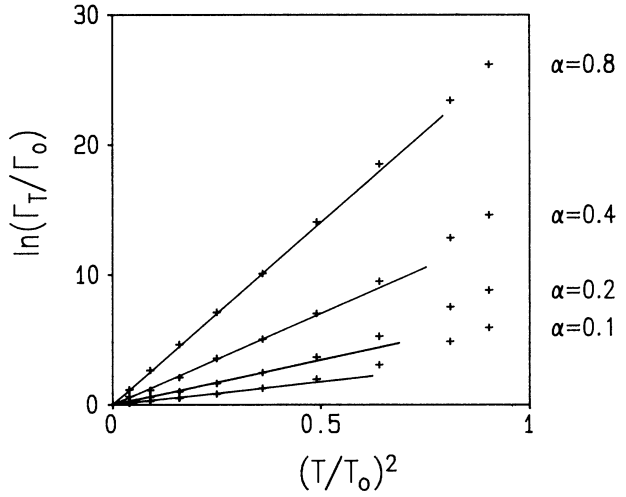

FIG. 11. The logarithm of the ratio of the finite temperature and the zero-temperature decay rate $\ln[\Gamma(\Theta)/\Gamma(0)]$ is shown as a function of the squared temperature ratio $T/T_0=\Theta/\Theta_0$ for a system with a cubic potential of barrier height $V_b=5\hbar\omega_0$ and various values of damping.

While we have given explicit results mainly for systems with a cubic potential and Ohmic dissipation the methods presented here can mostly be used also for systems with other forms of the potential and more complicated damping kernels. However, there are certain limitations of the approach which we shall shortly outline again.

Firstly, the process must occur under conditions of quasiequilibrium. This will be the case whenever the time scale of the decay is much larger than the relevant relaxation times determining the approach to the equilibrium distribution within the metastable well. This condition excludes highly underdamped systems where the relaxation processes within the well are not fast enough to balance the leakage across the barrier.[25,26] For temperatures above T_0 the relevant condition is $\hat{\gamma}(\omega_R)/\omega_b \gtrsim k_B T/V_b$. In the quantum regime the theory extends to even weaker damping because the tunneling rate remains finite for zero damping while the thermal hopping rate vanishes.

Secondly, the barrier height V_b must be large compared with other relevant energy scales. This is necessary because the functional integral for the partition function was evaluated in the semiclassical approximation. In the quantum regime the relevant condition is $\kappa \gg 1$ where κ is defined in (5.9), which amounts effectively to $V_b \gtrsim 5\hbar\omega_R$. In the classical regime the analogous condition reads $V_b \gtrsim 10\pi k_B T$.

Thirdly, we have assumed that the dynamic decay process can be described by one single rate. This condition can break down for low temperatures in cases where the potential has another well of comparable depth. Then the system may tunnel coherently between these wells. However, coherent oscillations are easily destroyed by environmental influences and finite temperatures so that this complication arises only for systems tunneling between two almost degenerate states and parameters within a small corner of the α-T plane.[41] For the most part, the dynamics of a damped double-well system can be described by a forward and a backward rate which may both be calculated by the method presented here.[42] Finally, the theory was based on the assumptions of linear dissipation and smooth potential shapes. Naturally, particular phenomena may arise from nonlinear couplings to the environment.

Langer's ImF approach is basically a thermodynamic method avoiding a fully dynamical investigation of the kinetic process. Clearly, there are a number of questions, such as the response to microwaves[43] and nonequilibrium effects that cannot be investigated within such a theory. A comprehensive description of the kinetic process can be based on the Feynman-Vernon theory.[44] This real time functional integral technique for damped systems has already been applied to particular problems in the theory of dissipative quantum tunneling[41] and is expected to allow for further extensions of the theory in the future.

ACKNOWLEDGMENTS

The authors wish to acknowledge stimulating discussions and helpful correspondence with S. Chakravarty, P. Hänggi, A. J. Leggett, and P. Riseborough. The completion of this work was greatly motivated by stimulating conversations with C. N. Archie, J. Clarke, M. H. Devoret, D. Estève, J. E. Lukens, J. M. Martinis, D. B. Schwartz, S. Washburn, and R. A. Webb. One of us (H.G.) is grateful to H. Müller-Krumbhaar for his kind hospitality at the IFF of KFA Jülich and to R. A. Webb for this generous support at IBM Research where important parts of this work were carried out. In addition H.G. would like to thank M. H. Devoret and D. Estève for their warm hospitality at Saclay where this work was completed. Financial support was provided by the Deutsche Forschungsgemeinschaft and by the European Community under Grant No. ST-2A-0200-F.

[1] A. J. Leggett, Progr. Theor. Phys. Suppl. **69**, 80 (1980).

[2] W. den Boer and R. deBruyn Ouboter, Physica **98B**, 185 (1980); R. J. Prance, A. P. Long, T. D. Clark, A. Widom, J. E. Mutton, J. Sacco, M. W. Potts, G. Megaloudis, and F. Goodall, Nature **289**, 543 (1981); R. F. Voss and R. A. Webb, Phys. Rev. Lett. **47**, 265 (1981); L. D. Jackel, J. P. Gordon, E. L. Hu, R. E. Howard, L. A. Fetter, D. M. Tenant, R. W. Epworth, and J. Kurkijärvi, *ibid.* **47**, 687 (1981).

[3] S. Washburn, R. A. Webb, R. F. Voss, and S. M. Faris, Phys. Rev. Lett. **54**, 2712 (1985); D. B. Schwartz, B. Sen, C. N. Archi, and J. E. Lukens, *ibid.* **55**, 1547 (1985).

[4] J. M. Martinis, M. H. Devoret, and J. Clarke, Phys. Rev. Lett. **55**, 1543 (1985); M. H. Devoret, J. M. Martinis, and J. Clarke, *ibid.* **55**, 1908 (1985).

[5] H. Grabert, U. Weiss, and P. Hanggi, Phys. Rev. Lett. **52**, 2193 (1984).

[6] H. Grabert and U. Weiss, Phys. Rev. Lett. **53**, 1787 (1984).

[7] H. Grabert, P. Olschowski, and U. Weiss, Phys. Rev. B **32**, 3348 (1985).

[8] A. J. Leggett, in *Percolation, Localization, and Superconductivity,* Vol. 109 of *NATO Advanced Studies Institute,* edited by A. M. Goldman and S. A. Wolf (Plenum, New York, 1984).

[9] H. Grabert, in *SQUID '85,* edited by H. D. Hahlbohm and H. L. Lübbig (de Gruyter, Berlin, 1985).

[10] P. Olschowski, H. Grabert, and U. Weiss (unpublished).

[11] A. O. Caldeira and A. J. Leggett, Phys. Rev. Lett. **46**, 211 (1981); Ann. Phys. (N.Y.) **149**, 374 (1983); **153**, 445(E) (1984).

[12] A. I. Larkin and Yu. N. Ovchinnikov, Pis'ma Zh. Eksp. Teor. Fiz. **37**, 322 (1983) [Sov. Phys.—JETP Lett. **37**, 382 (1983)].

[13] A. I. Larkin and Yu. N. Ovchinnikov, Zh. Eksp. Teor. Fiz. **86**, 719 (1984) [Sov. Phys.—JETP **59**, 420 (1984)].

[14] H. Grabert and U. Weiss, Z. Phys. B **56**, 171 (1984).

[15] L.-D. Chang and S. Chakravarty, Phys. Rev. B **29**, 130 (1984); **30**, 1566(E) (1984).

[16] D. Waxman and A. J. Leggett, Phys. Rev. B **32**, 4450 (1980).

[17] P. S. Riseborough, P. Hanggi, and E. Freidkin, Phys. Rev. A **32**, 489 (1985).

[18] E. Freidkin, P. S. Riseborough, and P. Hanggi, Z. Phys. B **64**, 237 (1986), and unpublished.

[19] E. Freidkin, P. Riseborough, and P. Hanggi, Phys. Rev. B **34**, 1952 (1986).

[20] P. Hanggi, H. Grabert, G.-L. Ingold, and U. Weiss, Phys.

Rev. Lett. **55**, 761 (1985).
[21]A. I. Larkin and Yu. N. Ovchinnikov, J. Stat. Phys. **41**, 425 (1985); A. I. Larkin, K. K. Likharev, and Yu. N. Ovchinnikov, Physica **126B**, 414 (1984).
[22]A. J. Leggett, Phys. Rev. B **30**, 1208 (1984); D. Esteve, M. H. Devoret, and J. M. Martinis, *ibid.* **34**, 158 (1986).
[23]Yu. N. Ovchinnikov and A. Barone (unpublished).
[24]E. Pollak, Phys. Rev. A **33**, 4244 (1986); W. Zwerger, Z. Phys. B 51, 301 (1983); V. I. Mel'nikov and A. Süto, J. Phys. C **17**, L207 (1984); A. Schmid, Ann. Phys. (N.Y.) **170**, 333 (1986).
[25]H. Kramer, Physica (Utrecht) **7**, 284 (1940).
[26]P. Nozières and G. Iche, J. Phys. (Paris) **40**, 225 (1979); M. Büttiker, E. P. Harris, and R. Landauer, Phys. Rev. B **28**, 1268 (1983); J. L. Skinner and P. G. Wolynes, J. Chem. Phys. **72**, 4912 (1980); B. Carmeli and A. Nitzan, Phys. Rev. Lett. **51**, 233 (1983); H. Risken and K. Voigtländer, J. Stat. Phys. **41**, 825 (1985).
[27]R. F. Grote and J. T. Hynes, J. Chem. Phys. **73**, 2715 (1980); P. Hanggi and F. Mojtabai, Phys. Rev. A **29**, 1168 (1982).
[28]B. Carmeli and A. Nitzan, Phys. Rev. A **29**, 1481 (1984); P. Hanggi and U. Weiss, *ibid.* **29**, 2265 (1984).
[29]For a recent review see P. Hanggi, J. Stat. Phys. **42**, 105 (1986).
[30]V. I. Gol'danskii, Dokl. Akad. Nauk SSSR **124**, 1261 (1959); **127**, 1037 (1959).
[31]J. S. Langer, Ann. Phys. (N.Y.) **41**, 108 (1967).
[32]I. K. Affleck, Phys. Rev. Lett. **46**, 388 (1981).
[33]For a recent critical discussion of Langer's method see, e.g., the paper by Waxman and Leggett (Ref. 16).
[34]P. G. Wolynes, Phys. Rev. Lett. **47**, 968 (1981); V. I. Mel'nikov and S. V. Meshkov, Pis'ma Zh. Eksp. Teor. Fiz. **38**, 111 (1983) [Sov. Phys.—JETP Lett. **60**, 38 (1983)].
[35]W. H. Miller, J. Chem. Phys. **62**, 1899 (1975); Adv. Chem. Phys. **25**, 69 (1974); M. Stone, Phys. Lett. **67B**, 186 (1977); C. G. Callan and S. Coleman, Phys. Rev. D **16**, 1762 (1977); S. Coleman, in *The Whys of Subnuclear Physics*, edited by A. Zichichi (Plenum, New York, 1979).
[36]R. P. Feynman, *Statistical Mechanics* (Benjamin, New York, 1972).
[37]H. Grabert, P. Olschowski, and U. Weiss, Phys. Rev. Lett. **57**, 265 (1986).
[38]The factor $\sqrt{2}$ arises because $\sqrt{2}\cos(\nu_n \tau)$ is normalized within the interval $\hbar\beta$.
[39]P. Olschowski (unpublished).
[40]A. N. Cleland, J. M. Martinis, and J. Clarke (unpublished).
[41]S. Chakravarty and A. J. Leggett, Phys. Rev. Lett. **53**, 5 (1984); A. J. Leggett, S. Chakravarty, A. T. Dorsey, M. P. A. Fisher, A. Garg, and W. Zwerger, Rev. Mod. Phys. **59**, 1 (1987); H. Grabert and U. Weiss, Phys. Rev. Lett. **54**, 1605 (1985); U. Weiss, H. Grabert, and S. Linkwitz, J. Low Temp. Phys. **68**, 213 (1987).
[42]H. Grabert and U. Weiss, Phys. Lett. **108A**, 63 (1985).
[43]M. H. Devoret, J. M. Martinis, D. Esteve, and J. Clarke, Phys. Rev. Lett. **53**, 1260 (1984).
[44]R. P. Feynman, F. L. Vernon, Ann. Phys. (N.Y.) **24**, 118 (1963).